"Short Proton-Induced Activities in Titanium and Iron"

A Thesis

Submitted in Partial Fulfillment of the Requirements for the Degree of Doctor of Philosophy in the Faculty of Graduate Studies and Research of McGill University.

by

Sydney W. Breckon, B.Sc.

April, 1951

TABLE OF CONTENTS

TABLE OF CONTENTS cont'd

TABLE OF CONTENTS cont'd

SUMMARY

Two new radioactivities of 0.40 and 0.18 seconds have been induced in titanium and iron targets respectively, by proton bombardment in the McGill University synchro-cyclotron. The threshold energies required for their production are approximately 9.5 and 13 Mev. By using an anthracene scintillation counter in a comparison method employing positron emitters of known energies, the radiations have been identified as positrons with maximum energies greater than 6 and $7\frac{1}{2}$ Mev., respectively. On the basis of the threshold energies, and on probable ft values of the positron transitions, the periods have been assigned to V^{46} and Co^{54} produced in the reactions Ti^{46} (p,n) V^{46} and Fe^{54} (p,n) Co^{54}. The bombarded targets were brought to a position outside the cyclotron by a quick-extraction process. The radioactive decays were observed by using a counting-rate meter in conjunction with a cathode-ray oscilloscope. Construction and operation of the equipment is described in detail.

I. INTRODUCTION

It was at the suggestion of Dr. J. S. Foster, Director of the Radiation Laboratory, McGill University, that the author undertook the study of short-lived radioactivities. As a result, a method for the examination of activities with second and fractional-second periods, has been developed, and two new periods discovered. The historical facts which led to a search for them, are described as follows.

Several years ago, G. R. Dickson and E. J. Konopinski[1] observed that families of odd-mass nuclei, differing from each other by α-particle units, show evidences of a certain type of regularity in their stability against β-processes. If one plots the logarithm of the half-life of each member of a family against its atomic number, the regularity becomes apparent by the way in which the members lie on a smooth curve. The assumption that a similar regularity held for all such families permitted the prediction of many radioactive periods unknown at that time. It is of interest to note that the predictions which have since met with the most success, were made with respect to the groups $Z = N+1$. Two families, one of Z-even and one of Z-odd, are present in this group. Known members of the Z-odd family are shown in Figure 1, where the logarithm of the half-life has been plotted against the atomic number. It is seen that the dotted curve extrapolation of the regular curve, gives a prediction of approximately 0.5, 0.4, and 0.3 seconds for the periods of the undiscovered members V^{45}, Mn^{49}, and Co^{53}.

Members of the $Z = N+1$ group are of special interest because, together with their $Z = N - 1$ isobars, they form Wigner

or 'mirror' pairs of elements[2]. Wigner pairs are nuclei such that one results from the other by interchange of neutrons and protons. Beta-transitions between them are super-allowed, and have ft values between approximately 1000 and 5000[2,3]. Furthermore these pairs are of interest because the difference between their binding energies may be attributed solely to the Coulomb energy of the 'extra' proton, if the assumption is made that the binding energy due to specific nuclear forces is the same for each member of the pair[4,5]. According to Barkas[6], the Coulomb energy is given by

$$E = 0.594\ (A - 1)\ A^{-1/3}\ \text{Mev} \qquad \ldots\ldots\ldots [1]$$

For β^{+}-transitions which go to the ground state, we may also write

$$E = E^{+}_{max} + 2e + (n - H) \qquad \ldots\ldots\ldots [2]$$

where E^{+}_{max} is the maximum energy of the positron spectrum, e the mass energy of the electron, and (n - H) the neutron-hydrogen mass difference in energy units.

It should be possible to produce the isotopes V^{45}, Mn^{49} and Co^{53} most conveniently, if at all, by (p,2n) reactions on the low mass isotopes, Ti^{46}, Cr^{50}, Fe^{54} of natural titanium, chromium, and iron respectively. This, together with the previous considerations, presented arguments in favour of a search for some of these periods. As a consequence, the author has studied specifically, the short period activities induced in titanium and iron by proton bombardment.

The methods used by experimenters to observe radioactive periods of the order of seconds, have been numerous and varied, depending to a large extent on the type of particle accelerator available, and on the internal or external nature of the beam. King and Elliott[7,8], who found Si^{27}, S^{31}, A^{35} and Sc^{41} of the Z = N+1 group, used an external beam from a cyclotron. They observed the

radioactive decay with a Geiger-Mueller counter, a scale of 16, and a mechanical recorder which was photographed every half second. In the technique employed by White et al.[5], an observer watching a Lauritsen electroscope which was detecting the short period radiations, actuated a moving-tape chronograph as the fiber shadow moved across the divided scale. Here again the target was bombarded outside the cyclotron, observations starting within 5 seconds after cessation of bombardment. A novel extension of their basic method was used by Schelberg et al.[9], who displayed Geiger-Mueller counter pulses on an oscilloscope tube, and photographed them together with time-marker pips, on a fast-moving film. They obtained a 0.58 second period in this manner which they assigned to Ti^{43}. Alvarez[10] in his studies on B^{8}, used the same principle by feeding the output pulse from a scaler to a moving pen recorder. His moving gate technique[11], in which he obtains the ionization being produced in a gated interval after the proton linear accelerator pulse has ceased, is limited to periods shorter than about 50 milliseconds, and was therefore not employed in this research.

In view of the considerable range of proton energies available in the McGill synchro-cyclotron*, resulting in a wide field for research, it appeared desirable at the outset of the work to develop a 'rapid survey' method of studying short period activities. By this is understood, a method which will allow an almost immediate estimate of a period to be made, and with some little further analysis, a value correct within 5% to be obtained. The development in recent years of fast electronic equipment, and of the scintillation counter[12,13] capable of counting at extremely high rates, has made it possible to

* The term synchro-cyclotron will hereafter be cited simply as cyclotron. The maximum energy of the McGill cyclotron is 100 Mev.

accomplish this aim.

In co-operation with W. M. Martin[14], equipment was constructed to work with the internal beam of the cyclotron. In the device, a pneumatic cylinder extracted a target-holding framework from within the cyclotron, bringing the activated target to a position just outside the main vacuum tank but still in the vacuum. Here the radioactivity was detected by a scintillation counter. The pulses from this were amplified and fed to a counting-rate meter via a pulse amplitude discriminator and scale of eight. The output from the counting-rate meter was displayed on a cathode-ray tube with a slow-sweep time-base. The picture thus obtained showed the radioactive decay directly, and could be photographed for a more careful analysis. A series of bright spots superimposed on the decay picture served as time markers.

In using this equipment, two new periods have been found. Titanium targets have yielded one, of 0.40 seconds, and iron targets the other, of 0.18 seconds. By using absorbers in conjunction with a thick anthracene crystal in the scintillation counter unit, it has been possible to estimate the nature and minimum energies of the radiations. Excitation curves have been obtained, and lead to approximate values of threshold energies for the reactions which give rise to these short activities. The results are discussed with particular reference to the assignment of the periods.

II. EXPERIMENTAL METHOD

A. Location of Counting Equipment

The first problem was to choose a suitable location for the counting equipment. It was clear that the target had to be irradiated inside the cyclotron tank, and might then be brought to a counting position outside. An alternative scheme of piping light pulses through lucite from a scintillation crystal located near the fixed target under bombardment, to a counter outside, offered too many difficulties. These arise, for example, from background activities in the ion current monitoring target, and from surrounding walls of the vacuum chamber. It thus became more attractive to move the target away from this confusing background before starting to count.

For this purpose, Schelberg et al.[9] used a 1/4" square pneumatic tube which projected into the cyclotron and terminated in an aluminium window. By air pressure, the target block was quickly drawn from its position at the window to a remote counting position in the laboratory. This method was scarcely suitable for the present study owing to the devious path of 150 feet from the Laboratory to the McGill cyclotron.

It was therefore decided to place the counter just outside the tank, so that the target could be brought quickly to this position. Magnetic shielding of the counter was achieved with multiple shields. The chief difficulty was due to background radioactivity, the greatest part of which came from the γ-radiation of Al^{28}, produced by the Al^{27} (n, γ) Al^{28} reaction in the aluminium magnet coils of the cyclotron. Fortunately, the short bombardments commonly used in this

work gave little opportunity for this activity to appear in appreciable strength. In a few unavoidable cases, however, where longer periods required longer bombardment, this background became a most disturbing factor.

B. Scintillation and Geiger-Mueller Counters.

The Geiger-Mueller counter has become such a common nuclear laboratory instrument that it needs no introduction here. S. A. Korff[15] has presented the important data on its properties and compiled a bibliography of the literature.

The Geiger-Mueller end-window β-counter has two distinctive properties which are sometimes advantageous in short half-life study as in other work; namely, a high efficiency for β-ray counting compared with that for γ-rays, and a uniform pulse amplitude output independent of the initial ionization. Because of the latter property, no pulse amplitude discriminator is required in its use. In spite of these advantages, the tube proves unattractive in the present application owing to a dead-time of several hundred microseconds which limits the counting rateof such an instrument to several thousand counts per second. Above this figure, counting losses become prohibitively large. It is clear that if such a limitation to counting rates exists, in the study of periods of less than one second, the total counts obtained will be small, and the statistics poor. Numerous repeated 'runs' can offset this disadvantage to a considerable extent, but the chance of other errors entering, due to variations in the 'runs', becomes much greater. The desirability of a fast counter for such work is obvious.

H. Kallmann[12] was the first to use photomultiplier tubes for the observation of light pulses produced in certain organic substances by ionizing radiations. In the last few years this method has been greatly developed by numerous experimenters[12,13,16-24]. In this so-called scintillation counter, light pulses from the irradiated crystal are allowed to fall on the photocathode of a secondary emission multiplier where they produce photoelectrons. These are multiplied by the tube, and give rise to pulses at the output. According to Morton[21], the gain of the average RCA 5819 tube, with 90 volts per stage, is about 6×10^5. The resolving time is about 10^{-8} seconds, the transit-time spread being less than this. Because of these qualities, the scintillation counter is capable of operating at high counting rates, yet gives voltage pulses of an amplitude easily handled by conventional electronic circuits.

Again, following Morton, one can estimate the size of the voltage pulses expected from an RCA 5819 with an output capacitance of, say, 10 $\mu\mu$fd. Let us assume that a 5 Mev β-ray dissipates its energy in the scintillation crystal. The crystal, producing one photon for each 50 electron volts of energy, gives 10^5 photons. If one assumes that 1/4 of these reach the photocathode, whose quantum efficiency is 6 per cent, then 1500 electrons will be released. Of these, about half will enter the multiplier. If the gain is 10^5, as was approximately the case in the work reported here, then a pulse of just under 3 volts will be obtained at the output.

Using high energy radiation, pulses of this magnitude were observed with the aid of an oscilloscope at the output of the multiplier. In comparison, the dark current pulses, which are characteristic of photomultipliers at room temperature, were very small.

The proportional nature of the photomultiplier has led to the measurement of γ-ray energies using NaI(Tl) crystals[22], and to the measurement of monoenergetic electrons in anthracene[24]. Hopkins[23,24] has found that the response of an anthracene scintillation counter to monoenergetic electrons, is linear from 125 kev to 1900 kev. Under ideal conditions, Ketelle has even been able to obtain a Kurie plot of the β-distribution of Ca^{45} [25].

For the detection of β-rays, anthracene has indeed proved to be one of the most efficient of the organic materials, and emits the light pulses with a decay time of 2.3×10^{-8} seconds[18,26,27]. Owing to the short resolving time of the photomultiplier, together with the possibility of measuring particle energies directly, an anthracene scintillation counter was chosen for this research.

C. The Counting-rate Meter Method.

In the measurement of short half-life activities, the scaler method of recording pulses consists in either, (a), photographing an electronic or mechanical indicator of a scaling device, at regular time intervals[7], or (b), recording on a moving tape or film, scaled pulses and time markers[9,10]. In both methods the inherent accuracy of the results is better than can be obtained by recording the output of a counting-rate meter[28]. However, the analysis of the second scaler method can become lengthy and tedious, particularly in the case of periods of less than one second, where the use of film is indicated. The first scaler method does not appear to be so easy to realize in practice.

The counting-rate meter method has, nevertheless, been used here in preference to either of the scaler methods, owing to

the quick manner in which a result can be obtained. It will be shown in Section III, however, that a high counting rate is necessary for the satisfactory operation of a counting-rate meter, so designed that it will follow a short period radioactive decay. Such high counting rates, on the other hand, only serve to increase the recording difficulties of the scaler methods. As will appear later, the counting-rate meter was well suited to the high rate of counting commonly realized in these experiments.

D. Determination of Positron Energies.

The cloud chamber method[8] of measuring the energies of positrons of short periods, could not be used with the experimental equipment as developed. For the same reason the gaseous target technique used by Perez-Mendez and Brown[29] in the study of He^6 with a beta-spectrometer, was not employed. The position and construction of the equipment was such that only two methods seemed practicable. One of these consisted in making energy measurements by the well-known absorption techniques[30,31]; the other, in using the proportional characteristics of the scintillation counter, in a manner similar to that used for the energy measurement of electrons.

The absorption technique for the energy measurement of positrons requires a counter with a good ratio of beta to gamma efficiencies, to keep the annihilation radiation count to a minimum. The scintillation counter, with a relatively high efficiency for gamma radiation, does not meet this requirement. The Geiger-Mueller counter, on the other hand, can, but the limitations it imposes on the counting rate, would have presented a serious handicap in the short-period work herein described.

Although measurements of electron energies have been made by experimenters, using anthracene crystals[23-25], the author was not able to find any reports on the measurement of positron energies made in a similar way. Such a measurement of positron energies is, of course, complicated by the presence of annihilation radiation, some of which is absorbed in the crystal by Compton collisions. In the case of anthracene, other absorption processes play but a small part. Using a relation given by Heitler[32] for the mean life of slow positrons in a material, one calculates a value of about 10^{-9} seconds for positrons in anthracene. Thus a pulse from a Compton recoil will, therefore, be unresolved from the pulse from the original positron.

According to Heitler[32], most of the positrons come to rest before being annihilated. However, some are annihilated while moving through the crystal, the probability being greatest when their kinetic energy is equal to the rest mass. In this case, the annihilation radiation will carry off the remainder of the positron kinetic energy, and will consequently possess an energy distribution of its own. Superimposed on this, will be the distribution in energy of the Compton recoils from those quanta absorbed in the anthracene crystal. The production of one-quantum annihilation radiation in anthracene should be so small as to be negligible.

W. M. Martin[14] has measured the integral bias distributions of several positron emitters, by detecting the positrons in an anthracene crystal. Using the published values for the maximum energies of these positrons, he has drawn up curves which

show a relation between certain points on integral bias distributions of positron emitters and the end-point energies. With his kind permission, the curves he obtained are reproduced in Figure 6. Points for these curves were obtained in the following manner.

A target of aluminium, for example, was mounted in the target-extractor unit (see section III) and subjected to repeated proton bombardments at regular intervals, to give, in this case, Si^{27} positrons. On each occasion, the short period activity was counted in two channels. In the first channel, the count was taken above a low fixed discriminator bias level. At the same time, in the second channel, a count was taken of pulses above a bias level which was varied between 'runs'. Let N_f represent the count in the fixed channel, taken over an interval of time long enough for the short period activity to have decayed; and let B_f represent the long period background and dark current count, taken in an equal interval and at a later time (corrected to zero time for any decay). Then $S_f = N_f - B_f$ is the count of the short-period pulses which are greater than the fixed bias level. Similarly, from the second channel, $S_x = N_x - B_x$ is the count of the short-period pulses which are greater than some bias x.

The count S_f was used to normalize the activities of the various 'runs', the normalized count for S_f being taken as 10,000. In this manner, normalized counts S_x were obtained for various discriminator bias settings. These counts were plotted semi-logarithmically against the discriminator bias, to give the integral bias curve shown in Figure 7 for Si^{27} positrons. The bias values at which this integral bias count is down by factors of 10^3 and $.5 \times 10^3$, have been taken as points representing different

degrees of cut-off of the composite spectrum of positrons and annihilation radiation. Such points taken for different positron emitters and plotted, discriminator bias against positron energy, give the curves of Figure 6. The x-axis intercept is interpreted as giving a mean energy value of the annihilation radiation absorbed in the crystal, and the y-axis intercept, as that discriminator bias at which the annihilation radiation would be down by the factor given by the curve.

The curves appear to be linear up to about 4 Mev. It is thought that the reason they start to show a saturation effect above this value, is because the crystal is too small to stop the high energy positrons.

The anthracene crystal used in these experiments was a rectangular parallelepiped of sides 1 1/4 x 1/2 x 1/2 inches, one of the small faces being placed toward the positron sources.

Comparison of points from the integral bias curve of an unknown positron energy with the curves of Figure 6, should permit one to make a reasonable estimate of this energy.

E. Counting Losses in Energy Determination Experiments.

In the previous section, the total number of pulses from a decay were deduced by scaling over a time interval long compared with the half-life of the decay. The treatment of counting loss corrections in this case, is set forth here.

If R represents a recorded counting rate, the counting rate corrected for losses will be of the form, $P = R + \alpha R^2$, and the fractional correction will be αR. If P is now considered to be a decaying rate, in which no counting losses occur, we have for

the accumulated count S, taken over a time t,

$$S = \int_0^t P\,dt = \int_0^t R\,dt + \int_0^t \alpha R^2\,dt.$$

For the case where $P \approx R$ we have

$$S \approx \int_0^t P\,dt + \int_0^t \alpha P^2\,dt.$$

The decay rate of a radioactive source is given by λN, where N is the number of atoms present, and λ is the decay constant.

Thus
$$S \approx \int_0^t \lambda N\,dt + \int_0^t \alpha \lambda^2 N^2\,dt$$

$$\approx N_o\left[-e^{-\lambda t}\right]_0^t + \frac{\alpha \lambda N_o^2}{2}\left[-e^{-2\lambda t}\right]_0^t$$

The exponential factors are small for

$$t \geq 5\,T_{\frac{1}{2}}. \qquad (T_{\frac{1}{2}} = \text{half-life})$$

Hence the fractional correction to the total recorded count is $\frac{\alpha(\lambda N_o)}{2}$. That is, the counting loss correction is one half that required for the initial counting rate. The initial counting rates of 'runs', taken for the energy measurement of radiation, were in general, less than 15,000 counts per second. The corrections thus amounted to less than one percent, and were neglected.

The method used for determining α is discussed in Section III.

F. Analysis of The Photographic Prints.

In order to obtain an accurate value of a period from the photographic recording, it was necessary first to print an enlargement of it, similar to that shown in Plate I. A line was then

drawn through the middle of the reference-line marker spots. In some cases a slight unevenness was present in the reference line. The cause of this was unknown, but it was found from experience that in this small section, the true base line was not represented by the marker spots. A smooth curve, which joined the remaining sections, served as a substitute.

It will be noted that in Plate I, the fluctuations of the counting-rate meter show up in a faint jittery trace. Where such a trace could be obtained by adjustment of the brilliance control, it served to indicate the mean line of the fluctuations of the counting-rate meter. It was through this mean value that a fine curve was drawn on the print. The distance between this line and the reference line was scaled at the position of the time-marker spots. Using a calibration print of standard signals, a calibration factor was obtained. From this, a value of the counting-rate was deduced, which was then corrected for counting losses. The long period background activity and photomultiplier dark current count, obtained immediately after the photograph had been taken, was subtracted from the corrected counting rate. Any decay of this background, appreciable enough to introduce errors of more than one per cent by its neglect, was corrected to zero time, and then subtracted.

Where no faint trace of the counting-rate meter fluctuations showed up, either because of a change of cathode-ray beam writing speed, or because of poor brilliance adjustment, the points were scaled from the reference line to the centre of the time-marker spots superimposed on the decay line. The counting-rate, determined by these methods of print analysis, was plotted semi-logarithmically

against time intervals determined by the time-marker spots. A corrected value of the frequency of these spots gave a corrected half-life value of the decay.

III. THE EXPERIMENTAL EQUIPMENT

A. General Remarks

The construction and design of the experimental equipment was undertaken in co-operation with W. M. Martin of the Radiation Laboratory, and many of its problems were subjects of discussion between us. In the main, however, Martin[14] was responsible for all control circuits, and certain other units of which specific mention will be made in the text.

B. Operation of the Equipment.

An understanding of the operation and function of the experimental equipment may be obtained, with the aid of the simplified schematic diagram, Figure 2, and of Plate III.

The target-extractor unit, hereafter designated TEU, rested on the cyclotron probe track and projected into the vacuum tank through the probe vacuum lock. The target to be irradiated by the proton beam, was attached to the front end of a small sliding holder which moved in a track in the TEU. This was connected to a variable stroke piston in the rear cylinder. The piston was motivated by compressed air controlled by the valve assembly, 16, and by the remote and main control panels, 17 and 18. As unit 1 did not provide damping action on the forward stroke of the piston, a constriction at a suitable place in the air valve assembly allowed a slow-injection quick-return motion of the target to be achieved.

After the target had been exposed to the proton beam of the cyclotron, it was quickly brought back to the counting position. This lay outside the vacuum tank, and away from the strong flux of

the cyclotron magnetic field. The target was held in position by the action of compressed air on the piston in the TEU cylinder; and an anthracene crystal and magnetically shielded RCA 5819 photomultiplier tube in unit 2, detected β and γ-radiations from it. A cathode follower circuit, 3, matched the output of the photomultiplier to the RG8/U cable transmission line. This carried the pulses to a linear amplifier, 4, at a position remote from the cyclotron room, and was terminated with 56 ohms. A discriminator and pulse shaper, contained in unit 4, passed all pulses above a selected bias voltage to a fast scale of 8, unit 6. Such a unit was necessary at this stage for fast counting, since the decade scaler, 14, had a resolving time longer than that of the discriminator. This discriminator, together with units 6 and 14, provided the variable bias channel described in Section II D.

The fixed bias channel consisted of a second discriminator and scale of 8, in unit 5. This unit was fed from the 'high level' output of the amplifier, the pulses having by-passed the discriminator of unit 4. A pulse shaping circuit received pulses from the scale of 8, and shaped them suitably for a counting-rate meter and a conventional decade scaler. The counting-rate meter, 8, contained one switch for selecting a particular short time constant integrating circuit, and another for selecting one of several sensitivities. The output of the counting-rate meter proper was amplified by a direct-coupled amplifier stage, and fed to the X plates of a cathode-ray tube in the oscilloscope, 19. A mechanically driven potentiometer in unit 10, produced a time-base[14], variable from about 3 to 30 seconds, by applying a voltage to the Y plates. Time-marker pulses from unit 9

were used to brighten the oscilloscope trace by means of a wide-band Z-axis amplifier, contained in the oscilloscope. The normal brilliance level of the trace was lowered so that these bright markers would stand out.

The radioactive decay of the target could be followed directly by observing the cathode-ray tube. At the same time it was possible to photograph the trace for a permanent record of the decay. In order to obtain a zero signal reference line on the photograph, the time-base generator was operated for one cycle, just before a 'radioactive run', and while the counting circuit was inoperative. The record was obtained on 35 mm film, and could be enlarged on printing, for easier analysis. An example of the result may be seen in Plate I, where the decay of A^{35} is shown. It may be noted here that it was also possible to obtain repeated time-base cycles during any radioactive decay, with successive record traces being photographed on the same 35 mm frame. Plate III illustrates the result of this method.

The extended-range unit, 12, controlled the scaling action of both decade scalers. A scale of 64, unit 13, operating off mains frequency, sent a pulse to unit 12, approximately every second. Consequently, pre-set counting intervals down to this value could be obtained. When the target came back to the counting position, all units started operating, and units 11 and 14 scaled for the pre-set interval. After the time-base on unit 19 had completed one cycle, the extended-range unit was reset, and the gross background activity followed until the period of its decay had been obtained. It is to be noted that all control circuits were quiescent during counting

intervals. Plate IV shows the equipment at the control position.

The radius at which the target was bombarded, could be varied by means of either the variable stroke adjustment at the rear of unit 1, or by the cyclotron probe controls which moved unit 1 as a whole along the probe track. Lights at the cyclotron control desk indicated the target to be at either the irradiation or counting positions.

The design of the control circuits[14] was such, that various methods were available for initiating action for the removal of the target from the cyclotron. Since all the short half-life measurements reported herein were carried out with pulsed operation[33] of the cyclotron oscillator, only the method applicable to these cases will be described in detail.

A beam monitoring block of copper, protruding beyond the probe nose of 1, allowed the cyclotron operator to monitor the cyclotron proton current, and adjust it to a specific value before the target was exposed. The sliding target holder was insulated from ground potential, thus providing for cyclotron tuning while the target was in the irradiation position. However, with experience, it was found that tuning in this position was unnecessary.

When the cyclotron had been readied for immediate operation, a trial burst of proton pulses was initiated by a switch on the oscillator pulser control unit. During this interval, the cyclotron beam current was tuned to a maximum on the copper block. When the tuning had been completed, the cyclotron oscillator was left OFF, but in the READY position, until the background radioactivity, which had built up during this relatively lengthy tuning period, had decayed to a low level. Now the time-base generator was operated for one

cycle, and a zero signal reference line generated for the photographic recording of the counting-rate meter output. At this time also, the target was moved into the cyclotron and the desired exposure period was set on the oscillator pulser control unit. At this point all equipment was ready for the bombardment to take place. With the flick of a switch on the pulser control unit, the target was exposed to the proton beam for the pre-set interval. At the end of this time the control unit shut off the oscillator, and energized circuits in the time-base generator, 10, which commenced operation, and thereafter took over control of the equipment by means of cams and micro-switches.

C. Details of the Apparatus.

1. Target-extractor Unit. (TEU).

Cross-sectional views of the probe and counter box assembly appear in Figure 3. In these views, some extraneous items have been omitted for clarity; for example, the bolts and nuts, parts 7, in the side elevation view.

The brass tracks, 15, in which the target holder moved, were held separated by brass supports, 13, spaced approximately every 6 inches along the length of the tracks. Around this track unit were fitted lucite rings, 17, also spaced 6 inches apart. These held the track unit centred in the stainless steel tubing of the probe. Longitudinal and rotational slip of the track was prevented by a heavy lucite ring, 9, which fastened both to the brass counter box, 10, and to heavy track-spacer blocks near the end of the box. The track was thus insulated electrically from the remainder of the probe. A small copper block, 18, which acted as a beam current monitor, was fastened

to the side of the track unit, and extended $3\frac{1}{2}$ inches beyond the end of the probe.

Both the front and rear parts of the probe tube, parts 4 and 14, were hard-soldered to brass flanges 12 and 19, which in turn were held to the box, 10, by stud bolts and nuts. Vacuum tight seals were made at these joints, as they were on the sides of box 10, by means of 3/16 inch square rubber gasket material, 5, fitted into appropriate gasket grooves.

Dural sides, 11, were clamped to the box, 10, by means of bolts and nuts, 7. In one of these sides a 3 3/4 inch hole, concentric with the target source position X, received the nose of the counter unit shown in Figure 5. An O-ring in a groove on the edge of this hole, provided a vacuum seal between the counter unit and box 10. An iron flange and tube, 23, was also fastened to this side, concentric with the hole. Part 23, shown again in more detail in Figure 5, acted both as magnetic shield and support for the counter unit.

Although seldom used, a lucite wheel, 6, for holding absorbers, 22, could be fitted inside box, 10, for carrying out absorber experiments. In fact, it was possible to fit two such wheels inside of the box, and rotate them independently on shafts, 8, which went through O-ring seals in the sides of the box.

Kover seals, 21, carried electrical wiring from the track and from micro-switch, 16, through the end of box, 10. Part 20 served to exclude light from the Kovar seals and hence the interior of the box.

Micro-switch, 16, closed when the target holder was in the front or target position and indicated this by means of a green light on the control panel.

The removable end of the probe, part 1, made a vacuum seal with the end of the stainless steel tube, 4, by means of an O-ring. Whenever the apparatus was assembled for experimental work, this block was removed, and the target holder inserted in the track. Block 1 was slipped over the stainless steel piston ram, part 42, Figure 4, and the target holder fastened to the end of the ram, 43, by means of a small stripper bolt. Two small O-rings maintained a vacuum seal around the ram. The block was screwed against the end ring, 2. This ring was grooved on the outside to take set screws from a tubular part, not shown, which served to align the probe end ring, 2, and the air cylinder end, part 34, Figure 4, and to keep them $1\frac{1}{2}$ inches apart.

The probe assembly was held in place by the probe carriage which supported ring, 3, by means of two dowel-ended screws. The front end of the assembly was supported by a small carriage which also was part of the cyclotron probe equipment. Both of these carriages may be seen in Plate III.

The target holder was moved by means of compressed air in the air cylinder assembly, shown in Figure 4. Air entered or escaped from the cylinder through the ports, 30 and 33, via a four way valve assembly. This air came from a remote compressor tank through 300 feet of $\frac{1}{2}$ inch copper tubing and 1 inch pipe. With a tank pressure of 90 pounds per square inch, the target could be extracted from the cyclotron in about $\frac{1}{4}$ second.

The piston ram was constructed from a thin wall stainless steel tube some 6 feet in length, which was sealed at one end by the plug, 43. A small collar soldered on the other end, was held between

the two parts, 39 and 40, of the piston. An O-ring in part 40, around the ram, kept the high pressure air from leaking inside it and working against the rapid extraction motion.

For adjusting the piston stroke, a $\frac{1}{4}$ inch diameter brass rod, 31, passed through the piston and into the hollow ram. This was capped by a special stainless steel nut, 41, held in place by a set screw, as well as threads. This nut moved freely inside the ram, but would not pass through the piston. Consequently it acted as a stop on the piston stroke. Adjustment was made at the rear of the end plug, 28, by means of two knurled nuts, 24, which moved the flat T end of rod,31,between a split and threaded steel tube, 25. This tube was brazed to the plug, 28. A total adjustment of $13\frac{1}{2}$ inches could be made in this manner. The piston, parts 39 and 40, was fabricated from dural, and had O-rings on the outside circumference to make a seal between it and the cylinder wall.

The backward motion of the piston was cushioned, by the piston nose building up air pressure in the right hand cup end of piece 28. Needle valve, 26, at the end of a small vent leading away from the cup, controlled the amount of cushioning. Air was prevented from escaping through other possible leaks, by means of O-rings. When the piston nose rested at the bottom of the cup, it pressed against the rod, 38, which opened micro-switch, 36, thereby closing the counting circuits. This action was indicated in the control room by a red light switching ON. Spring, 37, otherwise kept the micro-switch closed.

It was possible to adjust the target to coincide with the counting position X, Figure 3, (when the piston was against the end

plug, 28), by screwing 28 in or out of the end support ring, 29. When adjusted, part 28 was locked in position by the knurled nut, 27.

The end plug, 35, sealed the forward end of the brass cylinder, 32, the seal being made by an O-ring. The piston ram passed through another O-ring seal on the inside circumference of this piece, and a tubular nose on the inner end defined the limit of the longest stroke.

The tube (not shown) for aligning the cylinder with the probe, made a sliding fit over the end support ring, 34, and was held in place by set screws. Parts 34 and 29 were hard-soldered to the thin brass cylinder ends, and not only held the end plugs, but also contained manifolds for permitting rapid entry of air into the cylinder.

The cylinder was rubber mounted in a sliding carriage which moved on a track extension at the rear of the cyclotron probe track. This can be seen in Plate III.

The target holder which was attached to the front end of the piston ram, is shown in Plate V. The runners, and the central holder were constructed of dural, and were insulated from the brass piece which held the ram, by means of a bakelite block support. The overall length of the holder was $20\frac{1}{4}$ inches, and the target which was held in small jaws at the front end, as shown, was allowed to protrude an extra 1 3/8 inches.

An alternative form of holder was one in which the runners extended the whole length of $20\frac{1}{4}$ inches, and held the target between and beyond them for the extra 1 3/8 inches.

The assemblies described above allowed one to irradiate a target at any cyclotron radius from 10½ inches to 36 inches. With the incorporation of the control circuits[14], it was possible to

(a) count radiations from the target source in the normal counting position X; or

(b) count background radiations while the target was in the irradiation position in the cyclotron.

2. Scintillation Counter Unit.

A cross-sectional view of the scintillation counter unit is shown in Figure 5. Electronic components of the pre-amplifier have been omitted for clarity, but may be seen in a photograph of the opened unit in Plate VI. The unit, as shown, was mounted in the TEU, with its end extending through an O-ring seal in the side plate, 1. This plate, and the tube support, 2, are also parts 11 and 23 respectively, of Figure 3. The anthracene crystal, 3, fitted into the lucite light piper, 4, and was held in position by the lucite and by the aluminium foil, 5. This foil which covered the lucite, not only served to reflect light from the anthracene scintillations toward the type 5819 photomultiplier tube, but also to exclude from the tube, scattered light arising within the cyclotron vacuum tank. The conical end of the lucite piper fitted into a tapered brass seating ring, 6, and made a vacuum seal with it by means of an O-ring. The lucite was held in close proximity to the photomultiplier, 15, by means of a retaining ring, 7, which screwed against the seating ring. An O-ring seal between the seating ring and the shell of the counter, completed the vacuum barrier.

It will be noted that the anthracene crystal remained in the vacuum region. No serious difficulties were experienced from sublimation. To minimize this, all but the front surface of the crystal were covered with a thin layer of Canada balsam. This also filled small cracks and scratches in the crystal surface. After prolonged exposure, however, the front surface became slightly cloudy due to sublimation. This surface was easily refinished by polishing with cleansing tissue.

To protect the crystal from most background radiations, a block of lead, 8, was mounted round the end of the lucite piper. This lead piece contained a lucite lining, 9, which was inserted to prevent electrons produced in the lead by γ-rays, from reaching the crystal. Absorbers could be placed in the recess in front of this lucite lining. It should be mentioned that the absorber wheel, 6, Figure 3, could not be used with the particular crystal assembly described.

It is well known that the RCA 5819 photomultiplier is extremely sensitive to magnetic fields, and shows large variation in gain even for different orientations in the earth's magnetic field. Measurements in the fringing field of the cyclotron, taken in the median plane of the magnet, along the cyclotron probe direction, showed the zero magnetic induction point to be 8 inches beyond the outer circumference of the magnet coils. From this point out to 32 inches, a gradual increase to 170 gauss was noted. It was between these limits that the TEU could be moved. In general, however, the TEU was so adjusted that the counter remained in the low magnetic induction region.

The outer iron shell, 11, of the counter unit, and the inner

iron tube, 12, formed part of the magnetic shielding of the photomultiplier tube. For purposes of estimating a value of their combined shielding factor, these shells were treated as concentric cylinders with open ends. Using curves given by W. G. Gustafson[34] for infinitely long cylinders, and corrections for end effects in short cylinders, given by W. B. Ellwood[35], an estimated shielding factor of 168 was obtained. The shielding factor measured along the cylinder axes, 2 inches inside the front or 'detecting end', was found to be 262. The magnetic induction was thus less than 1 gauss, and it was considered that the μ-metal shield, 13, made by the John Millen Company, Malden, Mass., expressly for RCA 5819 photomultiplier tubes, would provide sufficient additional shielding.

The shields, 12 and 13, together with the rubber annulus, 14, formed a light trap inside the outer shell, to catch any light from the 6C4 tube at the base of the photomultiplier. In addition the 6C4 was coated with red glyptal to keep escaping light to a minimum.

A pre-amplifier designed by Martin[14], was assembled at the base of the photomultiplier and on the back plate of the unit. This matched the output of the photomultiplier to the 52 ohm coaxial transmission line which carried the pulses to the recording position 150 feet away. The pre-amplifier comprised a 6C4 in a phase inverter stage, and a cathode follower stageof two 6AG7 tubes in parallel. The bandwidth was about $4\frac{1}{2}$ megacycles per second.

The potential dividing resistors for the photomultiplier dynodes were also mounted beneath the tube base[14]. With a negative high-voltage supply of 945 volts, the voltages between successive dynodes from numbers 2 to 10, and from dynode 10 to

the collector, were 67.5 volts. Between the photocathode and dynode 1, there was 220 volts; and between dynodes 1 and 2, 130 volts.

High-voltage, and other cable leads were attached to plugs, 16, on the base plate, and to the cathode follower unit which plugged into the octal socket, 17. Forced air cooling for the electronic components was provided through the tubes, 18.

Experiments were carried out to ascertain to what extent the cyclotron magnet field affected the operation of the counter unit. In these, a Co^{60} source was placed in contact with the anthracene crystal, and the counter unit mounted in the TEU. With the cyclotron magnet current at its operating value of 625 amperes, the probe controls were adjusted to place the counter in the desired field. The amplifier gain was adjusted so that the integral distribution of the Compton recoils in anthracene, extended up to 90 volts discriminator bias. With this amplifier gain, the discriminator bias was set at 15 volts. It was noted that the counting rate dropped by $12\frac{1}{2}$ percent in the presence of the magnetic field. Orienting the counter unit by steps through 360 degrees, did not result in any changes greater than the probable error of measurement, which was about $\frac{1}{2}$ percent. In order to reduce the loss of $12\frac{1}{2}$ percent given above, to less than 3 percent, it was necessary to increase the magnetic shielding factor by incorporating an iron support, 2, Figure 5, as an integral part of the shielding. The iron annulus, 10, was also added at the end of the unit.

Although magnetic effects on the counter at 155 gauss,

were not entirely eliminated, the fact that the unit was kept in a low or zero magnetic induction region for all experimental work, permitted one to neglect them. Furthermore, they were small compared with the effect caused by attenuation in the coaxial transmission line, which reduced the counting rate by several percent.

The high voltage of the photomultiplier was varied while the counter unit was in the 155 gauss position described above. It was found that the unit was slightly more sensitive to changes in voltage with the field, than without it. Because of the stability of the voltage supply, this increase in sensitivity introduced but little additional uncertainty in results.

The entry of the charged particle component of the target radiation into the counter, was no doubt affected to some extent by the magnetic flux, even in the low induction region. The lower the energy of this radiation, the greater this effect. Provided, however, the magnetic field remained sufficiently constant, the effect introduced no error into measurements of half-lives of radiations. In the measurement of positron energies, only the very low energy component was affected appreciably, owing to the close proximity of the crystal to the source. The pulses from this component were too small to have been accepted, in any case, by the discriminators. Except for specific experiments on annihilation radiation, the low fixed bias level was set at 14 volts. Reference to the positron energy calibration curves of Figure 6, shows that a discriminator with 14 volts bias will reject pulses from positrons with less than 150 kev. of energy.

In addition to the crystal and lucite piper shown in

Figure 5, the following anthracene crystals were used, with suitable lucite pipers for assembly with the detector unit.

A. A hexagonal slab, $\frac{1}{2}$ inch thick and 1 inch across.

B. A thin cylindrical crystal, $\frac{1}{2}$ inch in diameter and 3/32 inches thick.

With crystal A it was necessary to use a different lead shield from the one already described.

The anthracene crystals were of high clarity, and practically free of cracks. Mr. A. Henrikson very kindly prepared these for the author. The mechanical construction of the counter unit was expertly done by machinists of the Laboratory.

3. Linear Amplifier and Discriminator.

An Atomic Instrument Company Linear Amplifier, Model 204-B, based on the design of Jordon and Bell[36], was used to amplify the pulses received from the coaxial transmission line.

Although performance data was supplied with the amplifier, tests were carried out on the wide bandwidth to ensure that the instrument was in good working order. It was on this bandwidth that the amplifier was used for scintillation pulses from anthracene. A simulated step signal with a rise time of 0.1 microseconds was applied to the input of the amplifier. The output pulse was found to have a rise time of approximately 0.2 microseconds, and a decay time of 0.4 microseconds. In this case, rise time is defined as the time required for the pulse to rise from 0.1 to 0.9 of the maximum, and decay time, as the time required for the pulse to decay from maximum to 0.1 maximum, when a step wave signal is applied to the input.

The gain on this bandwidth was approximately 3,500. Two adjustable attenuators at the input permitted one to obtain an overall

voltage attenuation of 36 decibels. The signal amplitude from the high level output was linear with respect to the input signal amplitude, up to a 100 volts at the output. The maximum noise output was found to be less than 1 volt at maximum gain.

A pulse amplitude discriminator, operating from the high level output of the amplifier, was an integral part of the unit. Pulses from the discriminator were found to vary in duration from about 1.0 to 2.2 microseconds, depending upon the relative amplitudes of the discriminator bias and triggering signal. The discriminator dial was calibrated, to give directly the amplitude of pulses which the discriminator just accepted. The amplitudes of these pulses were measured at the high level output. Thus adjusted, the dial gave readings of the high level output pulse amplitude to within $\pm$ 1 volt. The discriminator bias remained stable to $\pm \frac{1}{2}$ volt. A 6H6 diode D.C. restorer at the input of the discriminator, was removed for these measurements. Because of the rectifying action of this diode on pulse overshoot, and on negative noise pulses, it was left out for all the experimental work reported in this thesis.

The pulse shaping circuit at the output of the discriminator gave a pulse of 7 volts amplitude, and 0.5 microseconds duration. Under test, it was possible to pass a 1 megacycle per second pulse signal through the amplifier and discriminator.

A Tektronix type 511AD cathode-ray oscilloscope was used for observing the pulses described in the preceding paragraphs.

4. Counting-rate Meter.

The counting-rate meter was designed in co-operation with W. M. Martin[14]. In particular, Martin has analysed the conditions which must be applied in the design, if the counting-rate meter is to

exhibit an accurate reproduction of a short radioactive decay period.

An approximate limit on the period shortness which can be measured with the experimental equipment, will be set by the time taken for the TEU to bring the target source back to the counting position. A value of 1/4 second has already been given for this time. With an air reservoir in close proximity to the air cylinder assembly, no doubt this time could be reduced. In any case a 1/10 second period activity may be considered as the limit which could be measured.

Martin[14] shows that in a counting-rate meter used for measuring short period decays, the integrating time constant should be less than 1/10th the period of the activity being measured. He points out, as have Schiff and Evans[38], that the way in which the mean level of such a counting-rate meter follows the radioactive decay, is analogous to the behaviour of a short daughter radioactivity in transient equilibrium with a longer parent activity, which alone is present at zero time. This assumes, of course, that the charge on the integrating circuit of the counting-rate meter is zero, immediately before pulses from the radioactivity arrive. This was achieved in the present counting-rate meter, as will be seen later, by shorting the integrating circuit to ground through relay contacts which opened when the target source was in the counting position.

Under these conditions the output of a counting-rate meter reaches a transient equilibrium with the radioactivity in a time about twice the value of the integrating time constant. A continuous recording of the output, plotted semi-logarithmically against time, will yield a straight line in the equilibrium region, which gives very nearly, the period of the radioactive decay. However, the initial activity determined by extrapolating this line back to zero time,

does not give the true activity, but a value which is too high. For example, if a mean value of 0.6_2 (full scale) is obtained on the counting-rate meter, by injecting at the input a constant 10,000 pulses per second from a pulse generator, then under the transient conditions previously described, the counting-rate meter will show a mean value greater than 0.6_2 full scale, at a moment when the disintegration rate is 10,000 counts per second. The fractional error involved is a function of the time constant of the integrating circuit, and the period of the radioactive decay; the shorter the time constant, compared with the decay, the less the fractional error.

Where the value of the true initial activity is required, one can easily apply a correction obtained by referring to the case of transient equilibrium between radioactive decays[37].

Martin has also treated the case where more than one radioactivity is present. Here too, the result is that nearly true periods can be obtained from a recording of the output of the counting-rate meter, without applying corrections other than those normally required for separating two or more periods on a semi-logarithmic plot of activity vs. time. However, the initial activities determined from these plots are not only in error with the true activities, but the correction factors for each period are not the same. Again, these factors may be determined by referring to the transient equilibrium analogue.

So far, only the mean value from the integrating circuit has been considered. The accuracy with which one can determine this mean value from the recorded output of the counting-rate meter, will be determined by the fluctuations about this mean value, due to the

random arrival of pulses. Schiff and Evans[38] have treated the case for random pulses of constant width and amplitude. They find that the fractional probable error present in a reading of the counting-rate meter, due to fluctuations, is:

$$\epsilon = \frac{0.67}{\sqrt{2n\,RC}} \qquad \text{.....[3]}$$

where n is the counting rate, and RC the time constant of the integrating circuit. It has been shown[14] for the present counting-rate meter, that the minimum value of RC should be of the order of 10 milliseconds. Hence, to keep ϵ to 2 percent, for example, the counting rate should be approximately 56,000 counts per second.

From the conditions applying to counting-rate meters, as given by Elmore and Sands[39], and stated in a later paragraph, one immediately appreciates the difficulties in designing a counting-rate meter to accept such counting rates with small counting losses. The problem was simplified by reducing the pulses per second which the meter was required to accept. To accomplish this, a short resolving time scale of eight[14] was inserted before the counting-rate meter. This gave the statistical accuracy of the high counting rate, because of the smoothing action of the scaler on random pulses, and resulted in a more simple design of the counting-rate meter. For example, let us take 2 microseconds as the resolving time of the linear amplifier discriminator, a value which as we shall see, is nearly correct, and take less than 2 microseconds as the resolving time of the scale of eight. Then from nomographs given by W. C. Elmore[40] for computing fractional counting losses, it is apparent that for counting rates under 50,000 counts per second, the counting loss is practically independent of the resolving

time of the counting-rate meter pulse shaping circuit if it has a resolving time less than 50 microseconds. The loss which does occur, arises almost entirely in the pulse amplitude.discriminator of the amplifier, which has the assumed 2 microsecond, non-extended resolving time. Because of this, the lowest sensitivity range of the counting-rate meter was designed for 40,000 counts per second, full scale.

The diagram of the pulse shaping and counting-rate meter circuits is given in Figure 8. W. C. Elmore and M. Sands[39] list the inequalities which should hold in the basic counting-rate meter circuit as:

$$\left.\begin{array}{l} \frac{1}{n_1} \gg T > 5 R_0 C_{10} \\ E \gg V > E_{B1} \\ C_{1y} \gg C_{10} \end{array}\right\} \quad \ldots\ldots\ldots\ldots\ldots\ldots [4]$$

$$(y = 1, 2, 3)$$

where n_1 is the rate at which shaped pulses arrive at the integrating circuit of time constant $R'_{1x} C_{1y}$ $(x = 1, 2, 3, 4, 5, 6;\ y = 1, 2, 3)$. These rectangular pulses from the pulse shaping circuit have a duration T and an amplitude E. R_o is the internal resistance of this circuit as seen from the capacitor C_{10}. The other quantities are defined in Figure 8. Because of these inequalities, a charge $q = C_{10}E$ is deposited on the capacitance C_{1y} for each pulse, and the potential developed on the grid of V_7 by the integrating circuit is:

$$V = n_1 q R'_{1x} = n_1 C_{10} E R'_{1x} \quad \ldots\ldots\ldots\ldots [5]$$

$$(x = 1, 2, 3, 4, 5, 6)$$

for the case where n_1 remains constant. Because of the pre-scale of

eight unit, the value of n_1 for a counting rate of 40,000 counts per second, will be 5,000 pulses per second; i.e., $n_1 = \frac{n}{8}$.

The inequalities are well satisfied for the component values chosen. However, because of the voltage V developed across the integrating circuit, the charge deposited on the capacitance $C_{1\,y}$ per pulse, does not remain entirely constant and independent of V. From equation [5] it is evident that the charge is less than C_0E by the fractional amount

$$\frac{V}{E} = \left(n_1 R'_{1\,x}\right) C_{10} \quad \text{.....[6]}$$

For full scale deflection of the counting-rate meter, $n_1 R'_{1\,x}$ remains constant and independent of the sensitivity setting of the instrument. Hence the fractional error $\frac{V}{E}$ varies as the fractional full scale counting rate. Based on these considerations, the full scale error of the instrument of Figure 8, amounts to 1.3_5 percent.

The input pulse to the shaping circuit of Figure 8, is amplified by the triode-connected pentode, V_3. This tube is biased nearly to cut-off, thus preventing large negative overshoot on the pulse from interfering with the action of the univibrator circuit, designed around the triodes V_4 and V_5. Negative overshoot on the rectangular shaped pulses from the univibrator is clipped by the diode, V_6.

The basic circuit of the counting-rate meter, comprised of the capacitor C_{10}, the diodes V_1 and V_2, and the parallel resistance-capacitance circuit $R'_{1\,x}\ C_{1\,y}$, has been examined in detail by W. C. Elmore and M. Sands[39]. Switch, S_2, makes it possible to select one of four time constants; and switch, S_1, three sensitivities.

A cathode follower stage of nearly unity gain is inserted between the integrating circuit and the direct-coupled amplifier stage,

to reduce 'zero shift' which would otherwise be present on changing the sensitivity or time constant on the integrating circuit. Relay contacts, S_3, keep the grid of the cathode follower, V_7, at ground potential, until the counting-rate action begins. The output from the D.C. amplifier goes to the deflection plates of a cathode-ray oscilloscope, while the meter A_1, in the plate circuit of V_8 gives an approximate indication of the counting rate. The instrument may be set to zero by adjusting P_2 and observing the zero-point current on A_1. Owing to the short periods of operation, no high stability D.C. amplifier stage has been required.

A differentiating and clipping circuit consisting of C_7, R_{14} and the crystal diode, D_1, act as a pulse shaping circuit for a Berkeley Decimal Scaler.

The full scale sensitivities of the ranges of this meter, together with the selection of circuit time constants, are listed in Table 1, showing the probable error at full scale, in each case due to statistical fluctuations.

It was found in practice that a pulse of 10 volts amplitude, having a rise time of 0.05 microseconds, and an exponential decay, was satisfactory for triggering the univibrator. The pulse width from the univibrator was 7 microseconds in duration, and the resolving time for the circuit was estimated as being less than 20 microseconds. The D.C. amplifier was operated in the linear region of its characteristic curves; the voltage gain in this stage amounting to about 140. For 0.5 volts on the grid of V_8, a full scale deflection of 2 5/16 inches was obtained on the cathode-ray oscilloscope. To reduce drift in this stage, the filaments of V_7 and V_8 were heated by a 6 volt storage battery.

Calibration was carried out on all sensitivity and time constant ranges, using a pulse generator of variable frequency.

Table 1

INTEGRATING TIME CONSTANT (seconds)	0.016_5	0.014_2	0.10_3	0.25_8	SENSITIVITY
FULL SCALE COUNTING RATE (counts/sec.)	PERCENT PROBABLE ERROR				
40,000	1.8	----	----	----	
16,000	2.9	1.8	----	----	
6,400	4.6	2.9	1.8	----	
2,560	----	4.6	2.9	1.8	LOW
1,020	----	----	4.6	2.9	MED.
410	----	----	----	4.6	HIGH

On every combination of these two variables, the deflection of the cathode-ray tube beam was found to be linear with respect to the steady counting rate, within the accuracy of the measurements. This amounted to better than 2 percent over the greater part of the range. Calibrations were also carried out at the times of experimental runs, by photographing the counting-rate meter output from either a Co^{60} source of known counting rate, or from pulses of known repetition rate from a pulse generator. These were the calibrations used for analysing the photographic recordings.

On these photographs, no upswing of the counting-rate meter output was observed, which would give one the false impression of the presence of short period activity. Thus it was assured that no undesirable transient phenomena occurred in the counting-rate meter when S_3 opened.

Values of the circuit components of Figure 8 are given in Table 2.

Table 2

Resistors

R'_{11} - 33 K, ½ W, 1 Req'd.

R'_{12} - 82.5 K, ½ W, 2 Req'd.

R'_{13} - 206 K, ½ W, 3 Req'd.

R'_{14} - 516 K, ½ W, 3 Req'd.

R'_{15} - 1.29 M, ½ W, 2 Req'd.

R'_{16} - 3.22 M, ½ W, 1 Req'd.

R_2 - 10 K, ½ W

R_3 - 4.7 K, 2 W

R_4 - 180 K, 2 W

R_5 - 10 K, 2 W

R_6 - 220 K, 2 W

R_7 - 180 K, 1 W

R_8 - 9.1 K, 2 W

R_9 - 100 Ω, ½ W

R_{10} - 4.7 K, 1 W

R_{11} - 3.3 K, 1 W

R_{12} - 390 K, 1 W

R_{13} - 27 K, ½ W

R_{14} - 30 K, ½ W

R_{15} - 1 K, 2 W

R_{16} - 10 K, 1 W

R_{17}, R_{18} - 22 K, 2 W

R_{19} - Total - 105 K, 2 W

R_{20} - Total - 420 K, 1 W

Primed resistors are selected.

Potentiometers

P_1 - 2 K, 1 W

P_2 - 50 K, 4 W

Capacitors

C_2 - 500 μμfd.

C_3, C_6, C_9 - .01 μfd, 450 VW.

C_4 - 50 μμfd

C_5 - 50 μμfd, UHF

C_7 - 100 μμfd

C_8 - 8 μfd, 450 VW

C_{10} - Two 162 μμfd in series

C_{11} - 0.5 μfd, mica

C_{12} - 0.2 μfd, mica

C_{13} - 0.08 μfd, mica

Miscellaneous

S_1 - single pole, triple throw switch

S_2 - triple pole, quadruple throw switch

S_3 - relay contacts

A_1 - (0-1) milliameter

V_3, V_7 - 6AG5 tubes

V_4, V_5 - 6SN7 tube

V_1, V_2 - 6AL5 tube

V_6 - 6AL5 (one-half) tube

V_8 - 6AU6 tube

D_1 - 1N34 crystal diode

E_{B1} - C Battery 3 volts

E_{B2} - C Battery 7½ volts

5. Auxiliary Discriminator and Scales of Eight.

A pulse amplitude discriminator and pulse shaper, similar to that contained in the Atomic Instrument Co. Amplifier, was constructed by W. M. Martin[14] for the first channel. In addition, Martin has modified the basic scale of four circuit designed by Fitch[41], to give a scale of eight. The resolving time of this unit is less than 0.1 microseconds. Two such scalers were constructed. One of these was contained in unit 6 of Figure 2; the other in unit 5, along with the auxiliary discriminator.

6. Time-marker Generator.

The time-marker bright spots visible on the photographed recording of the counting-rate meter output, for example, in Plate I, were produced from small rectangular pulses amplified by the Z-axis amplifier of the Du Mont type 241 oscilloscope. Figure 9 shows the circuit diagram of the electronic time-marker generator, which supplied the rectangular pulses.

One of three repetition rates could be selected by switch S_1, viz, 2, 20, or 200 pulses per second. The 200 pulses per second were used chiefly to check electronic counting circuits. The pulse width was variable by means of potentiometer, P_8, from 35 microseconds with switch S_2 open; to 1.35 milliseconds with S_2 closed. No jitter in the time interval between the pulses on the 200 cycles per second range, was observed on a Du Mont type 208-B oscilloscope. In the case of the 20 cycles per second, jitter, if present, amounted to less than $\frac{1}{2}\%$ of the time interval. The amplitude of the pulses was variable up to 40 volts by means of potentiometer, P_7.

The unit remained stable over periods of several hours to within one part in a thousand on the high pulse rate; five parts in a thousand on the 20 pulses per second rate; and five parts in a hundred on the 2 pulses per second rate. The uncertainties in timing radioactive decay periods amounted to much less than the figures above would indicate, as the marker generator was calibrated against a synchronous clock at the beginning and end of each series of experiments. Corrections for the timing errors thus obtained, were applied to decay periods. On several occasions the 60 cycles per second mains frequency was checked against time signals from the United States Bureau of Standards radio station, WWV, over periods of eight hours. The mains frequency was found to remain within $\pm$ 0.1% of the stated frequency.

The marker generator was designed with the aid of standard circuit elements given by Elmore and Sands[39].

Examination of Figure 9 shows the first stage, based on the triodes V_1 and V_2, to be a symmetric multivibrator. Its frequency is changed by a change in some of the circuit RC time constants. Three pairs of ganged potentiometers, P_1P_4, P_2P_5, P_3P_6, make minor adjustments of the frequencies on the three separate ranges. Square waves from the anode of V_2 are differentiated by means of C_9 and R_{11}, the positive peaks being clipped by V_3. The diode, V_6, couples the negative pulses to the delay multivibrator or univibrator stage built around the triodes V_4 and V_5. The negative pulse triggers this circuit, and a positive rectangular voltage pulse appears at the anode of V_5. The width of this pulse is controlled by the RC time constant comprising R_{19}, P_8 and C_{12}, which is varied by the potentiometer, P_8. Wider pulses

are obtained by shunting C_{12} with C_{13} and R_{17}. Pulses from the univibrator may have a slight negative overshoot which is clipped off by the crystal diode X_1. The values of circuit components are given in Table 3.

Table 3

Resistors

R_1, R_2 - 50 K, 1 W

R_3, R_4 - 330 K, ½ W

R_5, R_8 - 3.3 M, ½ W

R_6, R_9 - 2.2 M, ½ W

R_7, R_{10} - 680 K, ½ W

R_{11} - 30 K, 1 W

R_{13}, R_{15} - 10 K, 2 W

R_{12} - 10 K, 1 W

R_{14} - 150 K, ½ W

R_{16} - 225 K, ½ W

R_{17} - 370 K, ½ W

R_{18} - 5 K, 1 W

R_{19} - 1 M, ½ W

R_{20} - 180 K, ½ W

Potentiometers

P_7 - 5 K, 1 W

P_8 - 8 M, 1 W

Double Potentiometers

P_1P_4 - 1 M, ½ W

P_2P_5 - 500 K, ½ W

P_3P_6 - 250 K, ½ W

Capacitors

C_1, C_6 - 0.025 μfd, 450 VW

C_2, C_5 - .0055 μfd mica

C_3, C_4 - 0.001 μfd mica

C_7, C_8, C_{14} - 25 μμfd

C_9, C_{12} - 100 μμfd

C_{15}, C_{10}, C_{11} - 0.01 μfd, 300 VW

C_{13} - 400 μμfd

Miscellaneous

S_1 - 4 pole, triple throw switch

S_2 - single pole, single throw switch

X_1 - 1N34 crystal diode

V_1, V_2 - 6SN7 tube

V_3, V_6 - 6H6 tube

V_4, V_5 - 6SN7 tube

7. Cathode-ray Oscilloscope and Camera Units.

A Du Mont type 241 cathode-ray oscilloscope was modified to take the output from the counting-rate meter on the X plates. One X plate was attached directly to the plate of the 6AU6 amplifier of the counting-rate meter, and the other went to ground via the X-shift control which was shunted by a 0.05 microfarad capacitor. To reduce the 'swinging time' of the oscilloscope, a 0.01 microfarad capacitor was used to shunt both the X plates and the shift control. This capacitor, together with the plate load resistor of the 6AU6, gave a time constant of about one millisecond. It proved desirable to have this value of time constant so that individual pulses arriving at the integrating circuit of the counting-rate meter, would not appear on the oscilloscope, but rather the mean integrated level plus fluctuations.

The time-base[14], generated by a motor driven potentiometer circuit, was applied to the Y plates. Time-marker pulses were applied to the Z-axis amplifier as explained previously.

A Du Mont type 314-A Oscillograph-Record Camera was used to photograph the radioactive decay on the face of the type 5JP11A cathode-ray tube. The unit may be seen mounted in place on the top and front of the oscilloscope in Plate IV. With the counting-rate meter disconnected from the X plates, it was possible to obtain a correct exposure on 35 microsecond duration time-marker brightening pulses, by using a lens opening of f2.8. About 80 such pulses, on a time-base extending over 2 3/4 inches of the tube face, could be resolved on the 35 mm film. However, when the counting-rate meter was applied to the X plates, the X-shift control had to be adjusted to an extreme position to balance out the standing potential of the

counting-rate meter amplifier. This unbalanced feeding considerably defocussed the spot. Consequently, for a proper exposure, 100 microsecond pulses with a lens opening f1.5, was required. Under these conditions about 50 pulses could be resolved on the film for the same extent of the time-base. This was entirely adequate for the experimental work undertaken.

Kodak Linagraph Ortho film was used as recommended by the Du Mont Laboratories.

8. High-voltage Power Supply

A conventional type of regulated high-voltage supply[21] was constructed for the 5819 photomultiplier tube on the basis of a transformer available from war surplus.

A single 2 X 2 half-wave rectifier tube fed a shunt condenser input filter. The output from this was regulated by a triode-connected 2E26 used as a series control tube, and a direct-coupled amplifier stage designed around a 6SJ7 tube. The supply was required to give about 1 milliamp, at from -900 to -1000 volts. However, because of the particular transformer used, the output voltage from the filter was over 1,600 volts on no load. Consequently, under certain operating conditions, the voltage across the control tube went as high as 600 volts. A 2E26 tube is designed for these voltages, and because of this was used in preference to some types more commonly used in regulated supplies.

Three VR150 regulator tubes were used to give a reference voltage for the D.C. amplifier.

The peak to peak ripple on the output of the regulated supply was less than 75 millivolts, and short period fluctuations

less than 100 millivolts. To periodically obtain an accurate check on the voltage, a 945 volt battery supply was used to back off the high voltage output. The difference voltage was read on a meter on the control panel. In fact, the regulated supply voltage was adjusted so that such measurements would draw but a few micro-amperes from the battery supply. It was found that under normal operating conditions the voltage drift over a period of several hours amounted to only a few parts in ten thousand.

At one time during the development of the experimental equipment, a relay was incorporated in the high-voltage line of the supply, so that voltage could be applied to the photomultiplier, only after the cyclotron oscillator had been shut off. Unfortunately, the closing of the relay contacts set up transient conditions in the circuit, which occasionally interfered with the stabilizing action. Because of this, the relay was finally removed, and the photomultiplier operated regardless of the state of operation of the cyclotron. No further difficulties were experienced with the supply.

A voltage of 945 volts was used on all the experimental work on short period activities.

D. Resolving Time of the Electronic Equipment.

The resolving times of individual electronic equipment units have been given in the previous sections. The interest here lies in the resolving time of the chain of electronic equipment in each channel. It is essential for the calculation of counting losses to know the value of this resolving time. Since the equipment pertinent to this discussion was the same for both channels, the treatment here will be made as if only one channel existed.

The introduction of a short resolving time scale of eight, between the pulse height discriminator and subsequent units of the channel, made the resolving time of the equipment almost entirely dependent on that of the discriminator. As noted before, the resolving time of the discriminator amounted to approximately 2 microseconds.

The general relationship between the recorded counting rate, R, and the 'true' rate, P, is assumed to be a power series of the form:(42)

$$P = R + \alpha R^2 + \beta R^3 + \gamma R^4 + \text{----------}$$

where α is the resolving time, and β, γ ---------- are independent parameters. The single parameter relation

$$P = R + \alpha R^2$$

has been taken as giving the 'true' counting rate with sufficient accuracy for our purpose.

The value of α can be determined by using the well known method of paired sources(42). If R_A and R_B represent the recorded counting rates of two radioactive sources of approximately equal strength, and R_C is the recorded rate of both sources taken together, then

$$\alpha = \frac{R_A + R_B - R_C - b}{R_C^2 - R_A^2 - R_B^2}$$

where b is the background rate.

The resolving time, α, was obtained using Co^{60} γ-ray sources. The amplifier gain was adjusted so that no output pulses were greater than 100 volts. The discriminator bias was set at 15 volts. The values obtained for α, using these methods, are given in Table 4, together with the combined counting rates R_C.

Table 4

R_C (counts/second)	α (seconds/count)
31,744	2.2×10^{-6}
28,124	2.59×10^{-6}
18,984	2.11×10^{-6}
6,765	2.26×10^{-6}

The mean of these values for α is 2.3×10^{-6} (seconds/count).

As an additional check on these measurements, a C^{11} β-ray source was followed for twelve half-lives, commencing with an initial counting rate of about 50,000 counts per second. When the dark current rate had been subtracted, the counting rate of the C^{11} activity was plotted semi-logarithmically against time. The application of counting loss corrections, based on the above figure for the resolving time, gave a straight-line plot, within the accuracy of the experimental measurements, over the entire decay[14].

It is to be noted that the value of α obtained in the manner outlined above, is close to the estimated resolving time of the discriminator. However, the possible effect of the 'pulse width' of the amplifier on counting losses must not be overlooked. There are a number of pulses present in an amplifier which are below the discrimination level, and will not be counted. However, as a result of the finite width of these pulses, and the random nature of their separation from one another, occasional 'piling up' will result. These 'pile-up' pulses may be passed by the discriminator as genuine pulses, and thus tend to give a false value to the recorded count. The short rise and decay times of the Atomic Instrument Ampli-

fier, however, kept 'piling up' to a low value at the counting rates used in these experiments. When integral bias distributions were being obtained, the counting rate was limited to less than 15,000 counts per second.

'Piling up' of pulses in the pre-amplifier, which had an input time constant longer than that of the main amplifier, has been discussed by Martin[14] in his treatment of the pre-amplifier design.

IV. EXPERIMENTAL RESULTS

A. Activity of the Target Holder.

The relatively slight activity induced in the aluminium target holder, by protons scattered from the target, was determined in the following experiments.

With the TEU in the operating position, the target holder was moved to a position beside the beam monitoring block of copper at the front end. Mounted on this block and 1 3/8 inches forward of it, was a platinum foil, 0.005 inches thick. Here the foil was almost in the same position relative to the aluminium target holder, as if it had been mounted directly on it in the normal manner. The platinum was bombarded for 15 seconds each run, at an energy of 34 Mev. At the end of the bombardment time, the holder was brought to the normal counting position, and the activity studied, the foil being left on the copper block. The only period found was about 5 seconds long. It was assumed that this was the 4.9 second activity of Si^{27} produced by the reaction $Al^{27}(p,n)\ Si^{27}$. The average initial counting rate amounted to 71 counts per second, compared with 3 counts per second from the gross background activity. Bombardment at 67 Mev. gave even less of the short activity with no measurable increase in the background.

The reduction of the above result to a bombardment time of 1 second gives a value of 10.5 counts per second for the initial activity. This counting rate is so low compared with initial rates of over 10,000 counts per second usually realized with targets, that it lies well within the errors with which these activities were measured. Its presence was therefore disregarded.

As additional evidence in this connection, it may be noted that quite accidentally, the above was confirmed. On several occasions during experimental runs, the targets were shaken free of a columbium supporting foil. Considerable long period activity had built up in some of these, because of repeated bombardments. With the holder in the counting position, the absence of any measurable activity above the gross background activity of the cyclotron room, indicated that these targets had been lost. These chance observations confirmed the results of the direct experiments, and showed that only trifling activity was induced in the target holder for target bombardments of the order of 1 second.

B. Half-life of A^{35}.

The overall efficiency of the experimental method was checked by comparing short period activities obtained in the manner described in this thesis, with values listed in the literature. W. M. Martin[14], using the same equipment as the author, obtained values of 0.87_3 seconds for the Sc^{41} activity, and 3.0_4 seconds for the Cu^{58} activity, in very close agreement with the published values of 0.87 seconds and 3 seconds[43].

The author, using a source of chemically pure $PbCl_2$ fused on a 0.005 inch thick columbium foil, obtained an activity identified as that of A^{35}, produced in the reaction $Cl^{35}(p,n)\ A^{35}$. Five runs have been analyzed and give values of 1.6_5, 1.6_7, 1.8_5, 1.7_3, 1.6_2 seconds, the mean being 1.7_0 seconds. Values of 2.2, 1.8_8 and 1.8_4 seconds have been given for this activity by White et al[44], Elliot and King[8], and Schelberg et al[9], respectively.

Both columbium and lead were examined separately, at the same

energy of bombardment, 13 Mev., for short period activities. No evidence of such activities was found.

In all but one instance (1.8_5 second period), the activity was followed for over four half-lives. The background activity (plus photomultiplier dark current count), was in no case greater than 0.08 percent of the initial counting rate of the 1.7 second activity.

A representative photographic recording from this group, run Cl-1-4, is shown in Plate I.

C. Short Period Activity Induced in Titanium.

Two titanium targets were bombarded with protons of various energies. One of these, designated Ti-2, was made of a double layer of 0.002_2 inch commercial grade foil. The double layer was necessary for rigidity in mounting the target in the holder, as shown in Plate V. The other target, Ti-3, was a fused lump of Hilger Spectrographic titanium, tied on a columbium foil with columbium ribbon. The titanium lump projected 1/4 inch beyond the foil, and when mounted, was about 1/2 inch in vertical extent.

Columbium foil was used to hold the target because it was found that even on direct bombardment at low energies, only a relatively low activity of long period was induced in it. Although photographic records of columbium, bombarded at 17.2 Mev., show some slight evidence of a low activity period of the order of 1 second, mounting the target as described above, prevented the proton beam from reaching the foil. As noted in Section IV A, this was confirmed on those occasions on which a target, mounted in this manner, inadvertently broke free.

An activity of 0.40 ± 0.01 seconds, was induced in the titanium targets at proton energies above 10 Mev. The above half-life is the mean

of seven values obtained from separate runs , the uncertainty being the standard deviation of these values from the mean. The seven, listed in Table 5, were chosen at random from first grade photographic records taken over a period of two months, during which time several modifications were made in the experimental equipment. These include a different scintillation crystal and pre-amplifier. A representative photograph, run Ti-2-12, is reproduced in Plate VII, and a semi-logarithmic plot of the activity versus time of run Ti-2-27, in Figure 10.

Table 5

Run Number	Proton Beam Energy (Mev.)	Bombardment Time (seconds)	Approx. Initial Activity (cts/sec.)	Background (cts/sec.)	No. of Periods Followed	Half-life (seconds)
Ti-2-12	22	2	57,000	1,600	5	0.38_7
Ti-2-27	22	1	29,000	283	4	0.40_5
Ti-2-40	22	1	18,500	725	3	0.39_3
Ti-3-9	$17._2$	0.5	12,000	72	4	0.39_8
Ti-3-10	$17._2$	0.5	14,000	83	5	0.41_9
Ti-3-13	$27._5$	0.5	42,000	149	5	0.41_1
Ti-3-14	$27._5$	0.5	42,000	206	5	0.39_8

Except for nitrogen (present in any case in some of the targets of other elements studied), the chief impurities given in the spectrographic analysis of Ti-3, were separately bombarded in target form to check that the activity was indeed induced in titanium, and not in an impurity. In addition, other elements were studied in the course of the experimental investigation. As a result, it can be stated that at a bombardment energy of $17._2$ Mev., and within the capabilities of the experimental equipment, no unknown short period activities[43] were ob-

served in the following target materials: Li, Be, C, O, Na, Mg, Al, Si, S, Cl, Ca, Cu, Ag, V, Pb. Of these, Mg, Al, Cu, V and Ag were of Hilger Spectrographic purity.

The relative yield of the 0.40 second activity as a function of the bombarding energy, is shown plotted in Figure 11. Some remarks are necessary concerning the method by which this curve was obtained. The integrated count (corrected for background activity), obtained by counting the short activity over the entire available decay, is proportional to the total atoms of short period activity remaining in the target when it reached the counting position. If one makes the assumption that the TEU brought the target out in the same time after each bombardment, then the values so obtained will give the relative amounts of the short activity induced in the target during various bombardments. The experimental observation that repeated runs at the same energy and bombardment time, gave the same amounts of activity within $\pm$ 10 percent, over a period of hours, indicates that this assumption is justified. However, an uncertainty arises between measurements made at different energies, as it was not possible with the experimental equipment at hand, to measure the cyclotron current during bombardment, with precision. Owing to the constancy noted above, and since the cyclotron was tuned at intervals to maximum ion current, it was assumed that the cyclotron operating conditions remained constant as bombardments were changed from one energy to another. Several runs were taken at most of the points plotted in Figure 11. The points were corrected to the same bombardment time, and for the decrease in proton current with increasing cyclotron radius. No account has been taken of the spread of energy in the proton beam. The energy values were taken from the Radiation Laboratory graph of cyclotron energy

versus target radius, calculated on the basis of the magnetic field strength, and not on actual energy measurements. At every plotted point except the lowest, direct photographic evidence of the short period activity was obtained concurrently with the other data. The uncertainties indicated are estimated probable errors. On the basis of these measurements, one can say that the threshold for the activity is certainly less than 11 Mev., and more probably about 9.5 Mev.

The target Ti-2 was also bombarded at 70 Mev. and three runs were analyzed. The periods of 0.42_0, 0.41_4, and 0.40_2 seconds show no definite evidence of any change from the 0.40 second obtained at low energies, within the probable experimental error. Using essentially the method described in Section II D, an integral bias distribution has been obtained for the annihilation radiation of Si^{27} positrons, stopped in a 10 Mev. thick copper absorber (6 mm. thick), mounted in front of the anthracene crystal. From this, the differential distribution shown in Figure 13 has been calculated, the bias voltages bearing a one to one correspondence with those in Figures 6 and 7. The steep part of the curve is interpreted as being the Compton edge of recoils in the anthracene, from the annihilation quanta. Points obtained in the same manner for the radiation from the 0.40 second activity, are plotted on the same graph. The standard deviations of the points have also been indicated. Within the limits of experimental error these points lie on the curve for positron annihilation radiation. Very little activity was observed to lie above a discriminator bias of 11 volts for either the Si^{27} or the 0.4 second activities. From the evidence, it appears that much, if not all, of the radiation from the 0.40 second period is associated with positrons.

To reduce the uncertainties in amplifier gain arising from

adjustment of the fine gain control, it was left unaltered during the whole series of experimental runs taken to obtain integral bias distributions. On this account, only the coarse gain control was used, giving adjustment by factors of 2. The points lying on the differential distribution were in fact, spread over much of the 100 volt bias range at the gain setting used. An increase of gain by a factor of 2 would have raised many of the pulses above the 100 volt level, and thereby caused saturation and blocking in the amplifier. This is the reason that more of the differential distribution at low bias levels has not been obtained.

A second integral bias distribution of the 0.40 second radiation was obtained, on this occasion without absorbers. It is shown as curve I in Figure 7, and may be compared with the distribution from Si^{27} positrons. The plotted uncertainties are standard deviations of the points. The integral count is down by a factor of 0.5×10^3 at a discriminator bias of 73.8 volts, and 10^3 at 77.0 volts. Transferring these values to curves I and II of Figure 6, gives points at L on the extrapolated portion of the curves. Martin[14] points out that there is considerable uncertainty attending his extrapolation to higher bias and energy values. However, taking this into consideration, it is reasonable to say that the positrons of the 0.40 second activity have a maximum energy greater than 6 Mev.

Points F are those obtained by Martin for a 0.28 second activity which he has observed on proton bombardment of chromium at energies above 13 Mev.

D. Short Period Activity Induced in Iron.

Two iron targets were also bombarded with protons of various energies. One of these, Fe-1, was made up of numerous strands of 0.01_0

inch diameter wire twisted together to form a small flat structure which projected 1 3/8 inches beyond the target holder. The wire was 99.8 percent iron. The other target Fe-2 was a $.004_5$ inch foil dry-rolled from a 1/4 inch diameter rod of Hilger Spectrographic iron. Prof. J. P. Ogilvie of the Metallurgical Engineering Dept. of McGill University, very kindly rolled this foil for the author. The foil was cleaned in nitric acid, and washed in distilled water. On proton bombardment at energies above 13 Mev., both of these targets exhibited a short period activity heretofore unobserved. The mean value of the half-lives from ten runs listed in Table 6, is 0.18 ± 0.01 seconds, the uncertainty being the standard deviation of the ten runs from the mean.

Table 6

Iron

Run Number	Proton Beam Energy (Mev.)	Bombardment Time (seconds)	Approx. Initial Activity (cts/sec.)	Background (cts/sec.)	No. of Periods Followed	Half-life (seconds)
Fe-2-33	$17._2$	0.5	6,800	52	5	0.18_4
Fe-2-38	$17._2$	0.5	9,500	65	5	0.18_1
Fe-2-32	$17._2$	0.5	7,000	52	4	0.20_6
Fe-1-30	$17._2$	0.7	12,000	129	5	0.19_5
Fe-2-69	$17._2$	0.5	13,000	102	4	0.17_8
Fe-2-70	$17._2$	0.5	9,000	108	5	0.18_6
Fe-2-72	$17._2$	0.5	11,500	102	4	0.16_9
Fe-2-78	$17._2$	0.5	12,800	78	5	0.17_6
Fe-1-8	$19._0$	0.5	3,800	346	6	0.17_3
Fe-1-9	$19._0$	0.7	5,180	310	5	0.17_8

The photographic record of Fe-1-30 is reproduced in Plate VIII

and the semi-logarithmic plot of the short period activity versus time, of Fe-2-70, in Figure 10.

The conditions under which the runs of Table 6 were taken, are similar to those described for the titanium runs of Table 5. The chief impurities listed in the spectrographic analysis of the iron of Fe-2 are included in the group of elements given in the previous section.

Analysis of the data collected from bombardments at 70 Mev., shows some evidence of a short period activity in addition to that mentioned above. Values of the additional unresolved period, estimated in each of three runs, are 0.25_0, 0.31_6 and 0.22_1 seconds, respectively.

The excitation curve of the 0.18 second activity from iron of natural isotopic constitution, has been derived in the same manner, and with the same uncertainties, as for that of the titanium activity. The excitation curve is shown in Figure 12. Here again, photographic evidence of the short period activity was obtained for all but the lowest point in the graph. The threshold almost certainly lies below 13 Mev., on the basis of the energy values of the graph. The curve above 30 Mev. has been shown as a broken line because it is not known where the threshold for the production of the second short activity lies, nor has it been possible to resolve the two activities. One point not shown plotted, at 60 Mev., lies at a relative yield of 7.

The differential bias distribution, deduced from the integral distribution taken with the 10 Mev. copper absorber in front of the anthracene crystal, is set forth in certain of the plotted points of Figure 13. These are to be compared with the distribution from the annihilation radiation of the Si^{27} positrons. At every point the standard deviation is such that the distribution of the radiation due

to the 0.18 second activity can be considered the same as for the annihilation radiation. There is no evidence of the presence of any radiation with energies greater than that from the annihilation radiation of the Si^{27} positrons.

The integral bias distribution taken without absorbers is shown as curve II in Figure 7. The integral count is down by a factor of 0.5×10^3 at $83._0$ volts bias, and 10^3 at $85._5$ volts bias. Here again one may place a lower limit to the maximum energy of the positrons by transferring these values to Figure 6. They are represented on curves I and II by the points at M. A reasonable lower limit may be considered as $7\frac{1}{2}$ Mev.

E. Measurements of the Energy of the Proton Beam.

The proton beam energy values used in compiling the experimental data, were calculated[45] from the relativistic formula

$$E = 938.3 \left\{ \left[1 + (0.8115_4 \times 10^{-6} BR)^2 \right]^{\frac{1}{2}} - 1 \right\} \text{Mev.}, \quad \ldots\ldots\ldots\ldots\ldots\ldots [7]$$

relating the proton energy E, with the magnetic induction, B (gauss), and the target radius, R (inches). This formula takes no account of factors arising from precession and oscillations of the proton beam. Therefore if the uncertainties in the measurements of thresholds are to be reduced, additional information on proton energies at various radii is needed.

W. H. Henry[46] has studied the characteristics of the beam precession and oscillations in some considerable detail at a calculated energy of 9 Mev. In the course of these experiments, he gave a short bombardment to an Ilford C 2 nuclear plate, placed edgewise to the beam

direction. Of over 700 proton tracks counted, not one showed an energy greater than 9 Mev. The broad peak of the energy distribution of the tracks extended to approximately 8 Mev.

In another experiment at the calculated energy of $8._2$ Mev., he placed various thicknesses of aluminium foil over a nuclear plate in a stepped fashion. This plate and foil combination was then exposed to the proton beam. It was found that none of the protons had passed through the $6._9$ Mev. thick foil. However, a considerable proportion had passed through the $3._4$ Mev. foil, and had darkened the plate. These results are essentially in agreement with those he obtained by observing proton tracks in the nuclear emulsion. He states that they are also in general agreement with results derived from his precession experiments.

The author carried out an experiment at a calculated energy of 13 Mev., similar to the one done by Henry with absorbers. In this instance, the aluminium foil and plate combination was mounted in the target holder of the TEU, and bombarded under conditions similar to those obtained in the work with titanium and iron targets. The result was that less than 0.01 percent of the beam passed through a foil $13._7$ Mev. thick for protons, and more than an estimated 5 percent through a 12 Mev. foil. The indications are that much of the intercepted proton beam is at energy lower than that calculated from the above formula, in rough agreement with Henry's results.

The uncertainties in energy of the points plotted in Figures 11 and 12, have been estimated on the basis of these measurements.

The values of the ranges of protons in aluminium were taken from the Berkeley Radiation Laboratory range-energy curves (1949)[47].

V. DISCUSSION OF THE RESULTS

A brief summary of the experimental results may be made as follows:

Two short half-life activities of 0.40 and 0.18 seconds have been induced in titanium and iron respectively, by proton bombardment. Within the limits of experimental error in the methods of investigation employed, the radiations from these periods appear to consist of positrons with maximum energies greater than 6 and 8 Mev. respectively. The threshold for the 0.40 second activity is in the vicinity of 9.5 Mev. proton energy, and that of the 0.18 second activity, less than 13 Mev. Not only do the radiations from the two activities appear very similar in character, but the reactions leading to them have threshold energies of roughly the same magnitude. This latter fact indicates that the reactions may be of the same type.

Reference to books and tables of nuclear data[43], indicates that the more common low energy proton reactions are (p, γ), (p,n), (p,p n), and (p,2 n), arranged in the order of increasing threshold energy.

All isotopes of both titanium, iron, and immediate neighbours which might be produced by (p, γ) and (p,p n) reactions are already well known. With one exception, this is also true of the less frequently observed (p,α) reactions, (Mn^{53}, close to the line of maximum stability and therefore likely to have a long half-life). By elimination, one is thus forced to consider the reactions (p,n) and (p,2 n) as more probable in the formation of the newly observed isotopes. From the threshold energies, one also reads that only the stable target isotope of lowest mass is involved.

In the introduction to this thesis, it was explained how predictions formed on the basis of the Konopinski observations, led the author to search for short periods in titanium and iron. Having found two such periods, it is natural to see whether or not they do indeed fit the predictions. Reference to Figure 1, shows two points marked I and II. These are the positions that the 0.40 and 0.18 second activities would take, if they were produced by (p,2 n) reactions. It is interesting to note that the 0.28 second activity which Martin[14] has observed on proton bombardment of chromium, lies at position III on the graph if a (p,2 n) reaction is also responsible for its production. The solid curve extension of the main curve, through these points, could be considered to be as good an extension as the dotted curve. Indeed, it would be the proper extension, if in fact, isotopes I, II (and also III) did lie at the positions marked. However, further examination of the experimental results, makes it extremely doubtful whether the points can be plotted in Figure 1 at all.

Table 7

EXPERIMENTAL			(P, 2 N) REACTION					
(a) HALF-LIFE OF ACTIVITY (SECONDS)	(b) ESTIMATED POSITRON ENERGY (MEV.)	(c) THRESHOLD ENERGY (MEV.)	(d) POSITRON ENERGY FROM [1] & [2]	(e) TARGET NUCLEUS	(f) PRODUCT NUCLEUS	(g) THRESHOLD FROM [8] & [9] (MEV.)	(h) f t VALUE	(i) TRANSITION
0.40	> 6	~ 9.5	5.5_8	Ti^{46}	V^{45}	20.6_4	930	super-allowed
0.18	> $7\frac{1}{2}$	< 13	6.5_1	Fe^{54}	Co^{53}	21.6_1	1800	super-allowed

In Table 7 are recorded some data pertinent to (p,2 n) reactions producing the observed periods. Columns (a), (b), and (c),

give some of the experimentally derived information. Column (d) gives the calculated positron end-point energy, using equations [1] and [2] for transitions between 'mirror' nuclei. The probable target nucleus is given in column (e), and the product nucleus of the reaction in (f). The threshold energy, E_T, for the (p,2 n) reaction in each case, is obtained from the relation:

$$E_T = 931 \left[M(A-1, Z+1) - M(A,Z) + (2n - H) \right] \frac{A+1}{A} \text{ Mev.} \quad \ldots\ldots [8]$$

where M is the nuclear mass, A and Z are the mass number and atomic number respectively of the target nucleus, and n and H are the neutron and hydrogen masses. The nuclear masses are obtained from the semi-empirical mass formula[48],

$$M(A,Z) = A - 0.00081\,Z - 0.00611\,A + 0.014\,A^{2/3} + 0.083\,(\tfrac{1}{2}A - Z)^2\,A^{-1} + 0.000627\,Z^2\,A^{-1/3} + \delta \quad \ldots\ldots [9]$$

$\delta = 0$ for odd A

$$= \mp \frac{0.036}{A^{3/4}} \quad \text{for A even} \quad \begin{cases} Z \text{ even} \\ Z \text{ odd.} \end{cases}$$

Substitution of (A - 1) for A, and (Z + 1) for Z, in equation [9], together with proper adjustment of the δ term for (A - 1) odd or even, gives the value M (A - 1, Z + 1). The threshold energy thus obtained from [8] is given in column (g). The f t value in column (h) was deduced, assuming a β^+-transition between ground states of nuclei, using the values of columns (a) and (d), and graphs of the function f (Z, W_0) set forth by Feenberg and Trigg[49]. The transitions, as noted in column (i), will be super-allowed because of the low f t values.

Two discrepancies between the experimental data, and the

assignment of the reaction to the (p,2 n) reactions listed in Table 7, appear in the positron energies, and the reaction thresholds. Although some uncertainty surrounds the experimental measurement of the energies, the experimentally obtained thresholds are far too much below the calculated values, for the difference to be bridged by any conceivable errors.

Table 8

EXPERIMENTAL			(P, N) REACTION					
(a) HALF-LIFE OF ACTIVITY (SECONDS)	(b) ESTIMATED POSITRON ENERGY (MEV.)	(c) THRESHOLD ENERGY (MEV.)	(j) POSITRON ENERGY (MEV.) (See p.63)	(e) TARGET NUCLEUS	(f) PRODUCT NUCLEUS	(k) THRESHOLD FROM [9] & [10] (MEV.)	(h) f t VALUE	(i) TRANSITION
0.40	> 6	~ 9.5	7.6_7	Ti^{46}	V^{46}	9.6_4	8400	super-allowed
0.18	> $7\frac{1}{2}$	< 13	8.3_4	Fe^{54}	Co^{54}	10.3_0	5400	super-allowed

Presented in Table 8 is a summary of data pertinent to a (p,n) reaction producing the observed short period activities. In each case, the threshold energy has been calculated from formula [9], and the relation

$$E_T = 931 \left[M(A, Z+1) - M(A,Z) + (n - H) \right] \frac{A+1}{A} \text{ Mev.} \quad \ldots\ldots\ldots [10]$$

Assuming a positron transition between ground states, the energy of column (j) has been calculated from the $M(A, Z+1) - M(A,Z)$ difference, and the relation

$$E^{max}_{positron} = 931 \left[M(A, Z+1) - M(A,Z) \right] - 1.01 \text{ Mev.}$$

It will be noted in the case of the (p,n) reactions, that both the calculated positron energies and the threshold values lie within reach of the experimental values. The f t values of 8400 and 5400, deduced from columns (a) and (j), make the transitions super-allowed[49].

Such transitions also fit in with the (p,n) reaction scheme. Wigner[4] has treated the case of β-transitions between isobars with N = Z (odd), and (N - 2) = Z (even), (N and Z not the same in each case). The ground states of these nuclei belong to the same Wigner supermultiplet[50], and the transitions may be interpreted as going between $^1S_0$ and $^3S_1$ ground states with nearly identical space wave functions. Three such transitions are[49], $He^6 \rightarrow Li^6$; $F^{18} \rightarrow O^{18}$; $A^{26} \rightarrow Mg^{26}$. The proposed transitions $V^{46} \rightarrow Ti^{46}$ and $Co^{54} \rightarrow Fe^{54}$ thus satisfy the Wigner conditions. If ground state transitions do occur between these nuclei; then from the exceptional overlap of wave functions, one should expect them to be super-allowed. In this case no γ-rays from excited states would be present. This, too, coincides with the experimental observations on the short period radiations.

It thus appears that (p,n) reactions are indeed the ones responsible for the short period activities. Therefore one can tentatively assign the 0.40 second activity to V^{46} induced by the Ti^{46} (p,n) V^{46} reaction, and the 0.18 second activity to Co^{54} induced by the Fe^{54} (p,n) Co^{54} reaction.

The position of the half-lives on the Dickson-Konopinski graph thus appears to be coincidental. It may be that (p,2 n) reactions in Ti^{46} and Fe^{54} do give short period activities which may even be slightly longer than the ones obtained, thus fitting more closely to the dotted curve extension of Figure 1.

One is encouraged to accept this view by the persistence of strong activity (0.40 sec.) in titanium under bombardment up to 70 Mev., and by the appearance of a longer activity in the iron target under similar bombardment.

VI. ACKNOWLEDGEMENTS.

The author takes pleasure in acknowledging the guidance of Professor J. S. Foster, F.R.S., Director of the Radiation Laboratory. Professor Foster not only suggested to the author that the investigation of short period radioactivities would prove to be of great interest, but also during the ensuing research, encouraged him with interest and advice.

Apart from the many beneficial discussions which naturally take place between co-workers, the author wishes to thank Mr. W. M. Martin for his assistance during the operation of the experimental equipment. In this connection also, Mr. R. H. Mills has rendered whole-hearted co-operation during long tedious hours spent in obtaining experimental data.

The author is pleased to acknowledge the help received during interesting discussions with Dr. J. D. Jackson, particularly with reference to theoretical aspects of assignment of the short period activities; and with Dr. C. H. Westcott.

At the outset of the experimental work, Mr. J. D. Keys and Mr. W. H. Henry very kindly showed the author how the cyclotron pulsing equipment could be used to the best advantage. In addition, the author is grateful to Mr. Henry for communicating to him the results of his experiments on the measurement of the proton beam energy.

Mr. S. R. Doig, foreman of the machine shop, and his staff, deserve credit for the skillful manner in which they fabricated the many mechanical parts associated with the equipment.

Many additional members of the Radiation Laboratory have con-

tributed in one way or another to the work reported in this thesis. In the main, these were: Dr. A. L. Thompson, who assisted in the preparation of some of the targets; Mr. A. Henrikson, who prepared the anthracene crystals; Mr. P. B. Troup, who gave advice in connection with some of the electronic circuits; and Mr. Mills and Mr. J. F. Mathison, who assisted in the preparation of the drawings and photographs. The author gratefully acknowledges the assistance which these research workers have given him.

In addition, the effort spent by Dr. J. P. Ogilvie in the preparation of one of the iron targets, is much appreciated.

VII. BIBLIOGRAPHY

(1) G.R. Dickson and E.J. Konopinski, Phys. Rev. 58: 949 (1940).

(2) E. Fermi, "Nuclear Physics", (The University of Chicago Press, Chicago, 1950), p. 83.

(3) L.W. Nordheim, Phys. Rev. 78: 294 (1950).

(4) E. Wigner, Phys. Rev. 51: 947 (1937); Phys. Rev. 56: 519 (1939).

(5) White, Delsasso, Fox and Creutz, Phys. Rev. 56: 512 (1939).

(6) W.H. Barkas, Phys. Rev. 55: 691 (1939).

(7) L.O.P. King and D.R. Elliot, Phys. Rev. 58: 846 (1940).

(8) D.R. Elliot and L.O.P. King, Phys. Rev. 60: 489 (1941).

(9) Schelberg, Sampson and Mitchell, Rev. Sci. Inst. 19: 458 (1948).

(10) Luis W. Alvarez, Phys. Rev. 80: 519 (1950).

(11) Luis W. Alvarez, Phys. Rev. 75: 1815 (1949).

(12) H. Kallmann, Natur und Technik, July 1947.

(13) M. Deutsch, Phys. Rev. 73: 1240 (1948).

(14) W.M. Martin, Ph.D. Thesis, McGill University (1951).

(15) S.A. Korff, "Electron and Nuclear Counters" (D. Van Nostrand, New York, 1946).

(16) F.H. Marshall and J.W. Coltman, Phys. Rev. 72: 528 (1947).

(17) R.J. Moon, Phys. Rev. 73: 1210 (1948).

(18) P.R. Bell, Phys. Rev. 73: 1405 (1948).

(19) J.W. Coltman, Proc. Inst. Radio Eng. 37: 671 (1949).

(20) H. Kallmann, Phys. Rev. 75: 623 (1949).

(21) G.A. Morton, R.C.A. Review X: 4, Dec. 1949.

(22) R. Hofstadter and J.A. McIntyre, Phys. Rev. 78: 619 (1950).

(23) J.I. Hopkins, Phys. Rev. 77: 406 (1950).

(24) J.I. Hopkins, Phys. Rev. 79: 415 (1950).

(25) B.H. Ketelle, Phys. Rev. 80: 758 (1950).

(26) Gittings, Taschek, Ronzio, Jones and Masilun, Phys. Rev. 75: 205 (1949).

(27) R.F. Post and N.S. Shiren, Phys. Rev. 78: 80 (1950).

(28) A.G. Bousquet, Nucleonics 4: No. 2, 25 (1949).

(29) V. Perez-Mendez and H. Brown, Phys. Rev. 77: 404 (1950).

(30) E. Bleuler and W. Zunti, Helv. Phys. Acta XIX: 375 (1946).

(31) N. Feather, Proc. Cambridge Phil. Soc. 34: 599 (1938).

(32) W. Heitler, "The Quantum Theory of Radiation" (Oxford University Press, London, 1944), p. 204.

(33) W.H. Henry and J.D. Keys, Can. J. Phys., to be published.

(34) W.G. Gustafson, Bell System Tech. J. 17: 416, July (1938).

(35) W.B. Ellwood, Bell Lab. Record 17: No. 3, 93, November (1938).

(36) W.H. Jordan and P.R. Bell, Rev. Sci. Inst. 18: 703 (1947).

(37) Rutherford, Chadwick and Ellis, "Radiations from Radioactive Substances" (Cambridge University Press, London, 1930), p. 11.

(38) L.I. Schiff and R.D. Evans, Rev. Sci. Inst. 7: 456 (1936).

(39) W.C. Elmore and Matthew Sands, "Electronics: Experimental Techniques" (McGraw-Hill Book Co., Inc., New York, 1949),

(40) W.C. Elmore, Nucleonics 6: No. 1, 26 (1950).

(41) V. Fitch, Rev. Sci. Inst. 20: 942 (1949).

(42) T.P. Kohman, MDDC - 905, June 13, 1945.

(43) "Nuclear Data," Circular of the National Bureau of Standards 499, (Sept. 1, 1950)

(44) White, Creutz, Delsasso and Wilson, Phys. Rev. 59: 63 (1941).

(45) F.A. Johnson, Radiation Laboratory, McGill University.

(46) W.H. Henry, - private communication to the author.

(47) Aron, Hoffman, and Williams, AECU Document 663 (UCRL 121).

(48) C.F. v. Weizacker, Z. Physik 96: 431 (1935);

cont'd

(48) N. Bohr and J.A. Wheeler, Phys. Rev. 56: 426 (1939); reference (2) p. 7.

(49) E. Feenberg and G. Trigg, Rev. Mod. Phys. 22: 399 (1950).

(50) L. Rosenfeld, "Nuclear Forces" (Interscience, New York, 1948), p. 200.

LEGEND FOR FIGURE 2

1. Target-extractor Unit
2. Scintillation Counter
3. Cathode Follower Unit
4. Linear Amplifier and Discriminator
5. Auxiliary Discriminator and Scale of Eight
6. Scale of Eight
7. Pulse Shaper
8. Counting-rate Meter
9. Time-marker Generator
10. Time-base Generator
11. Decade Scaler
12. Extended-range Unit
13. Scale of 64
14. Decade Scaler
15. High-voltage Supply
16. Air Valve Assembly
17. Remote Control Panel
18. Main Control Panel
19. Cathode-ray Oscilloscope

LEGEND FOR FIGURES 3 AND 4

1. Probe End Plug
2. Probe End Ring
3. Probe Support Ring
4. Probe Tube --- Rear
5. Rubber Gaskets
6. Absorber Wheel
7. Bolts and Nuts for Counter Box
8. Absorber Wheel Shafts
9. Main Lucite Ring
10. Counter Box
11. Counter Box Sides
12. Probe Tube Flange --- Front
13. Track Supports
14. Probe Tube --- Front
15. Tracks
16. Micro-switch --- Front
17. Lucite Rings
18. Beam Current Monitoring Block
19. Probe Tube Flange --- Rear
20. Shield for Kovar Seals
21. Kovar Seals
22. Absorbers
23. Counter Support and Shield
24. Lock-nuts
25. Stroke Adjustment Tube
26. Needle Valve
27. Lock-nut

28. Cylinder Plug --- Rear
29. Cylinder End Ring --- Rear
30. Port --- Rear
31. Stroke Adjustment Rod
32. Cylinder
33. Port --- Front
34. Cylinder End Ring --- Front
35. Cylinder Plug --- Front
36. Micro-switch --- Rear
37. Spring
38. Micro-switch Rod
39. Piston
40. Piston
41. Stop Nut for Part 31
42. Piston Ram
43. Ram Plug

LEGEND FOR FIGURE 5

1. Counter Box Side
2. Counter Support and Shield
3. Anthracene Crystal
4. Lucite Piper
5. Light-reflecting Foil
6. Seating Ring
7. Retaining Ring
8. Radiation Shield
9. Lucite Lining
10. Magnetic Shield --- Front
11. Counter Shell and Shield
12. Inner Magnetic Shield
13. Mu-metal Shield
14. Light Excluder
15. RCA 5819 Photomultiplier
16. Electrical Connectors
17. Octal Socket
18. Tubes for Air-cooling.

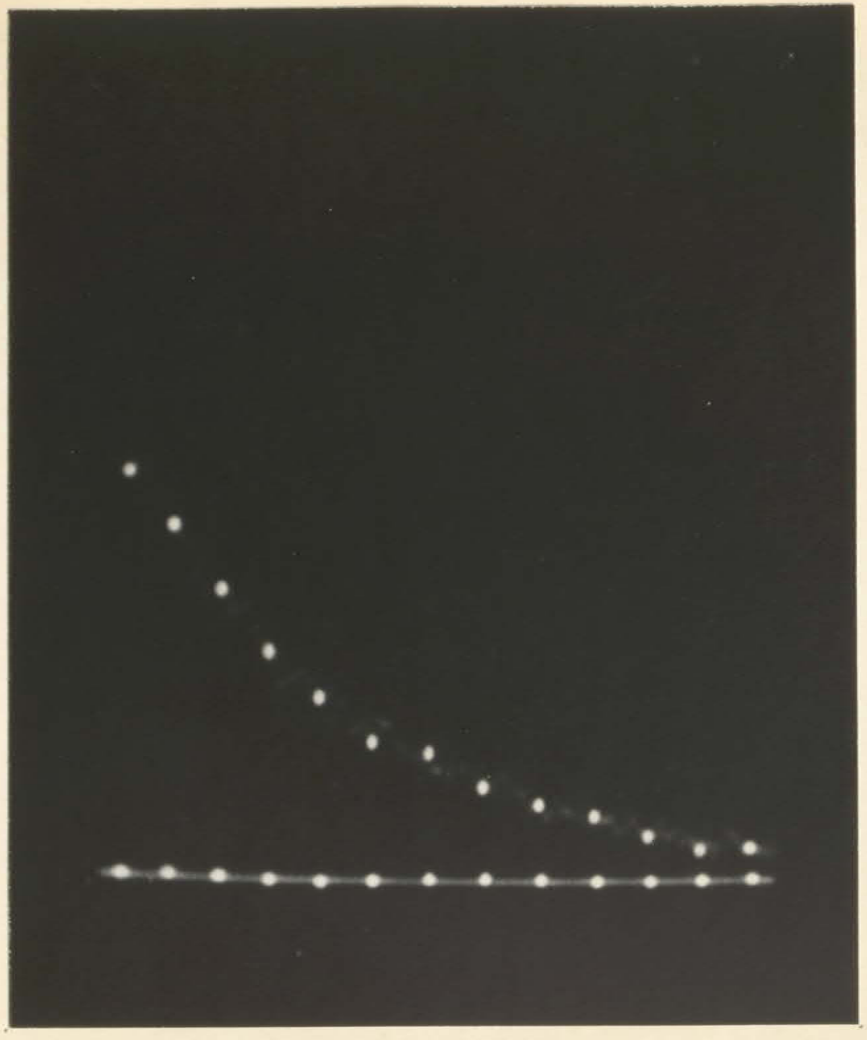

Decay of A^{35}

Run Cl-1-4; half-life 1.6_2 sec.;
time-marker spots 1.95/sec.

PLATE I

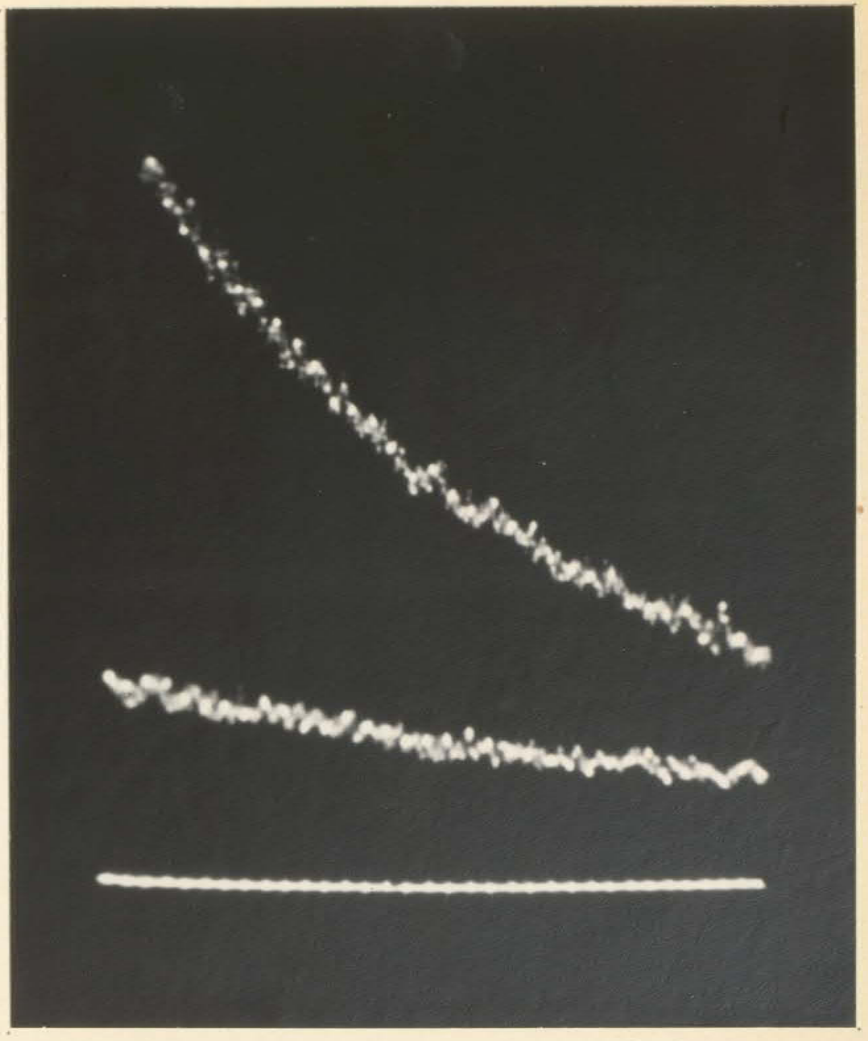

Decay with Repeated Time-base

Two cycles plus zero signal reference line are present.

PLATE II

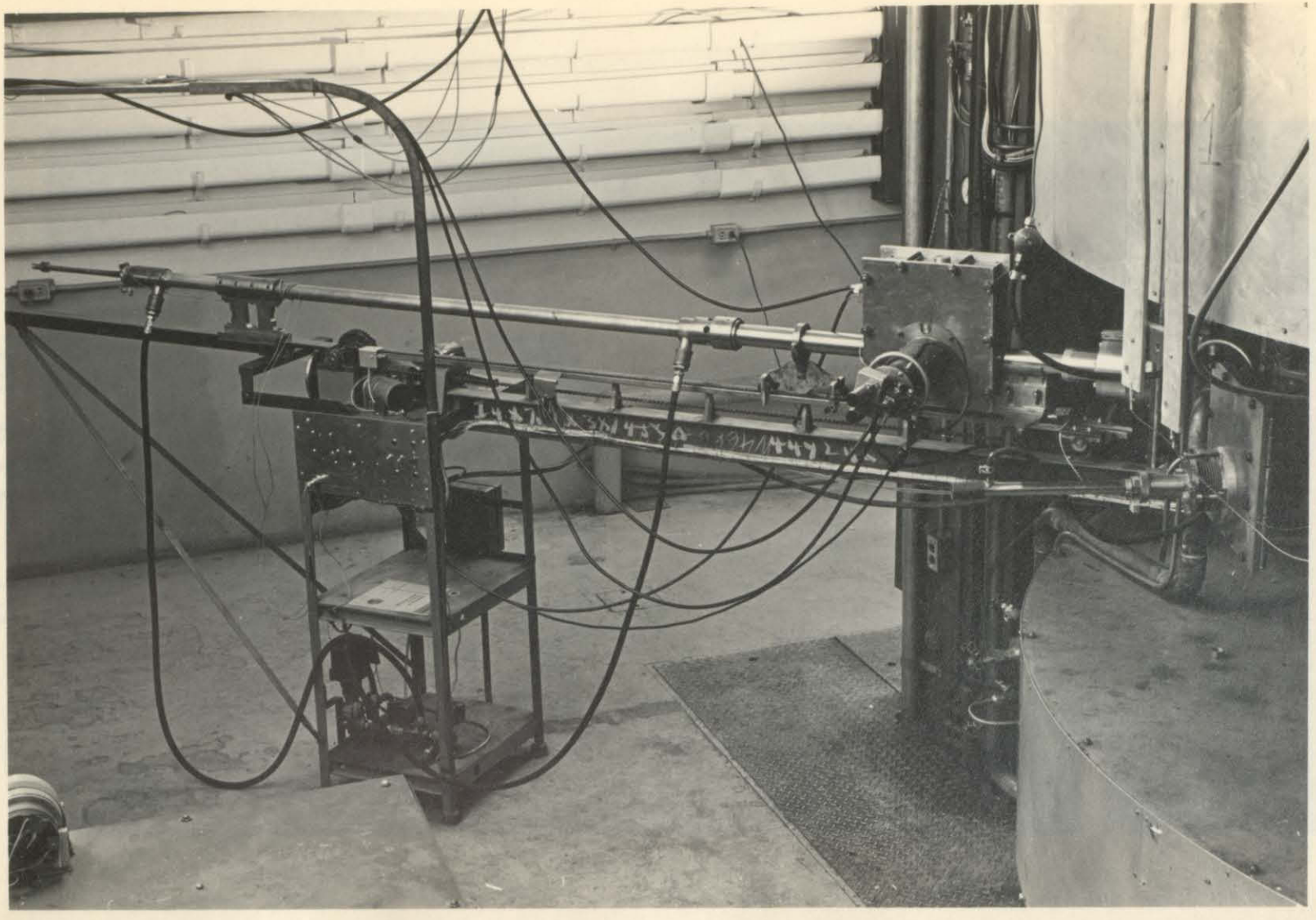

PLATE III

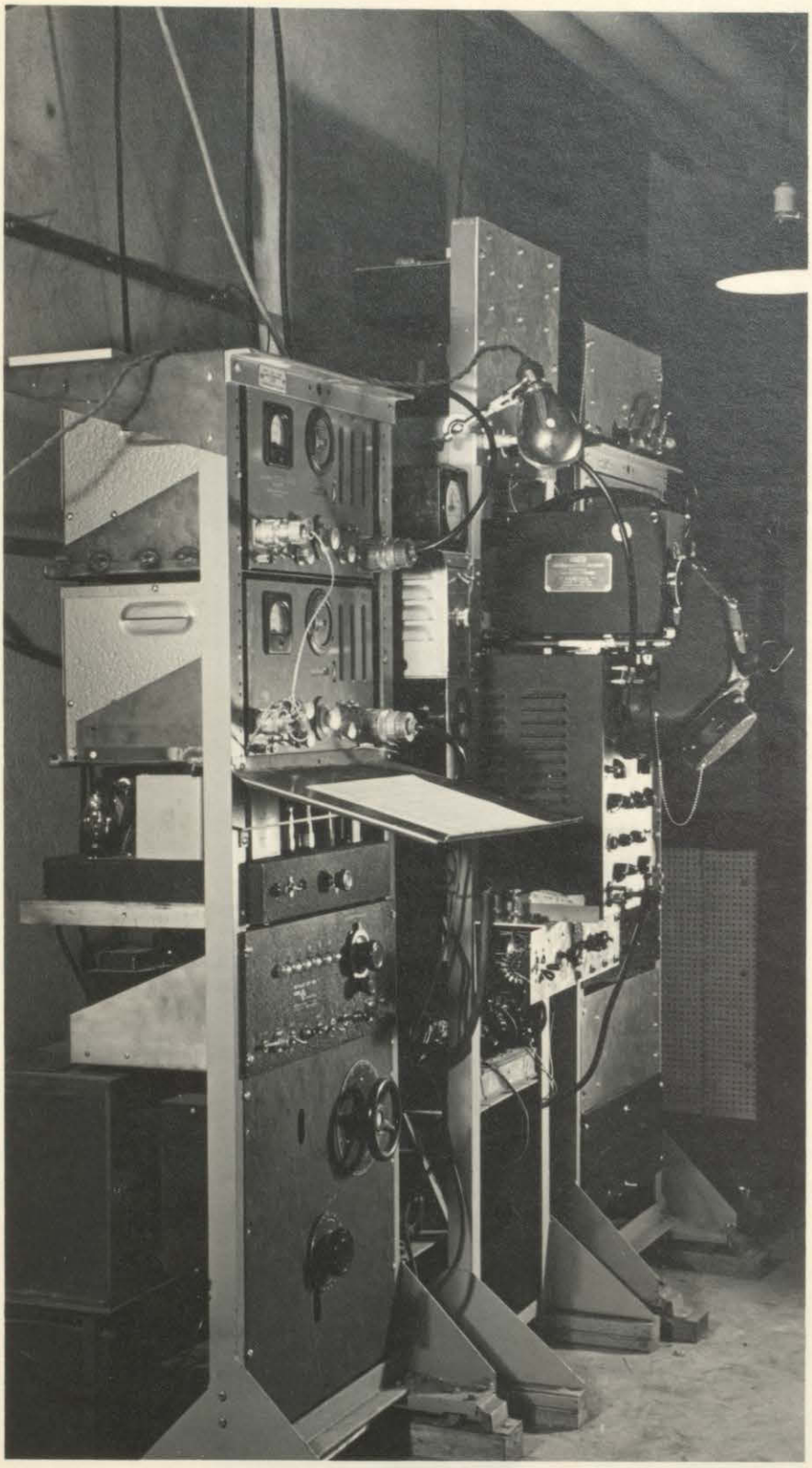

PLATE IV

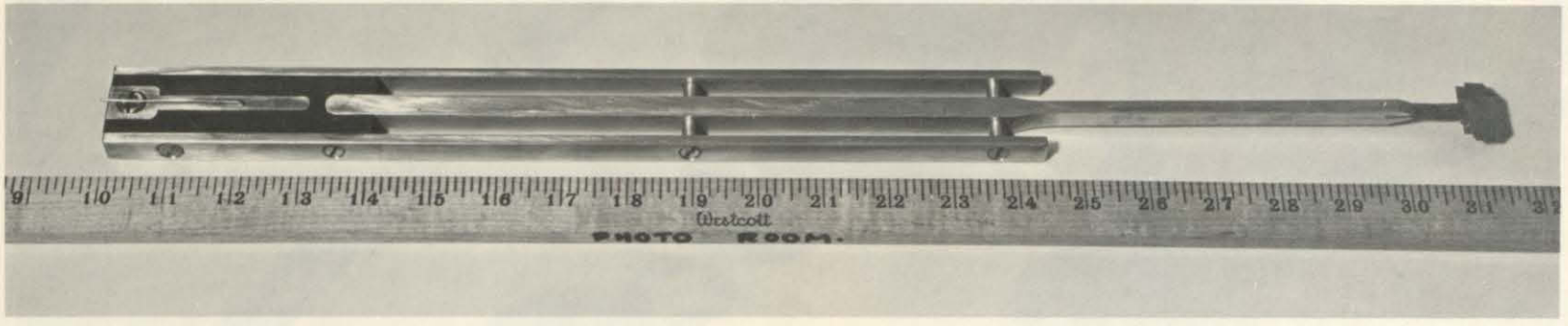

PLATE V

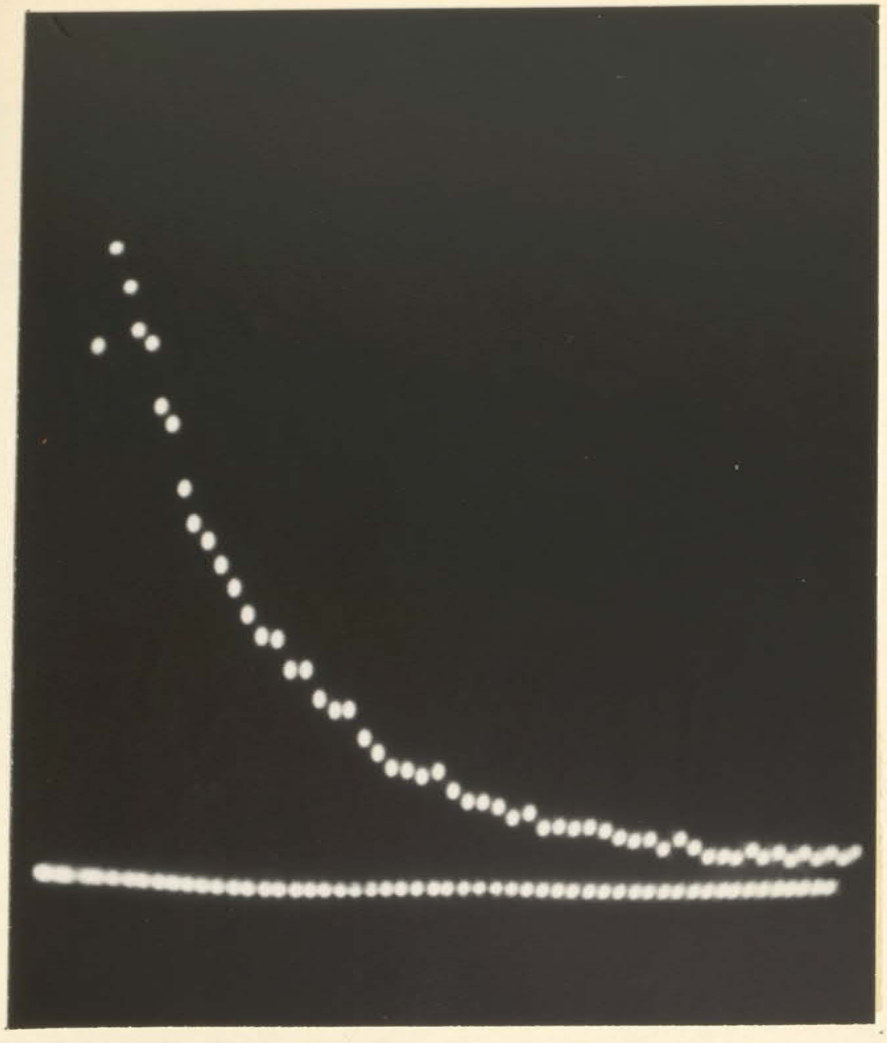

Decay of Activity Induced in Titanium

Run Ti-2-12; half-life 0.38$_7$ secs.;
time-marker spots, 20.26/sec.

PLATE VII

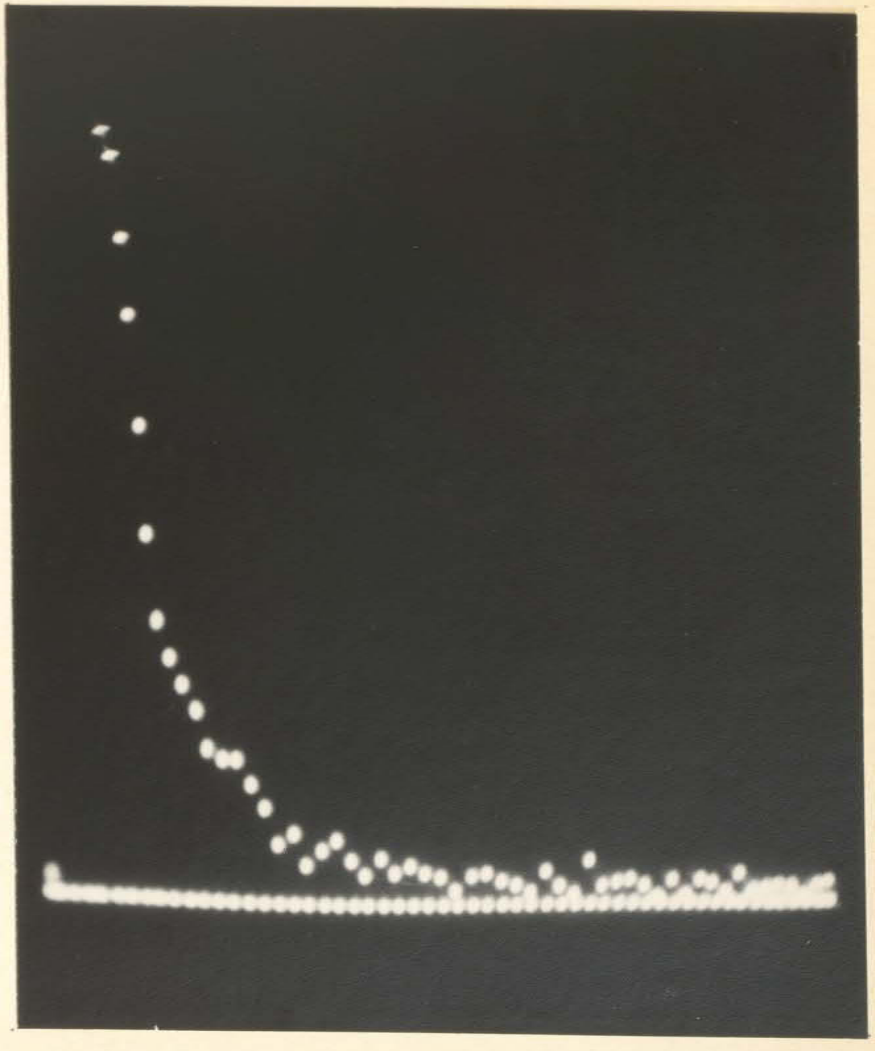

Decay of Activity Induced in Iron

Run Fe-1-30; half-life 0.19$_5$ secs.;
time-marker spots, 20.15/sec.

PLATE VIII

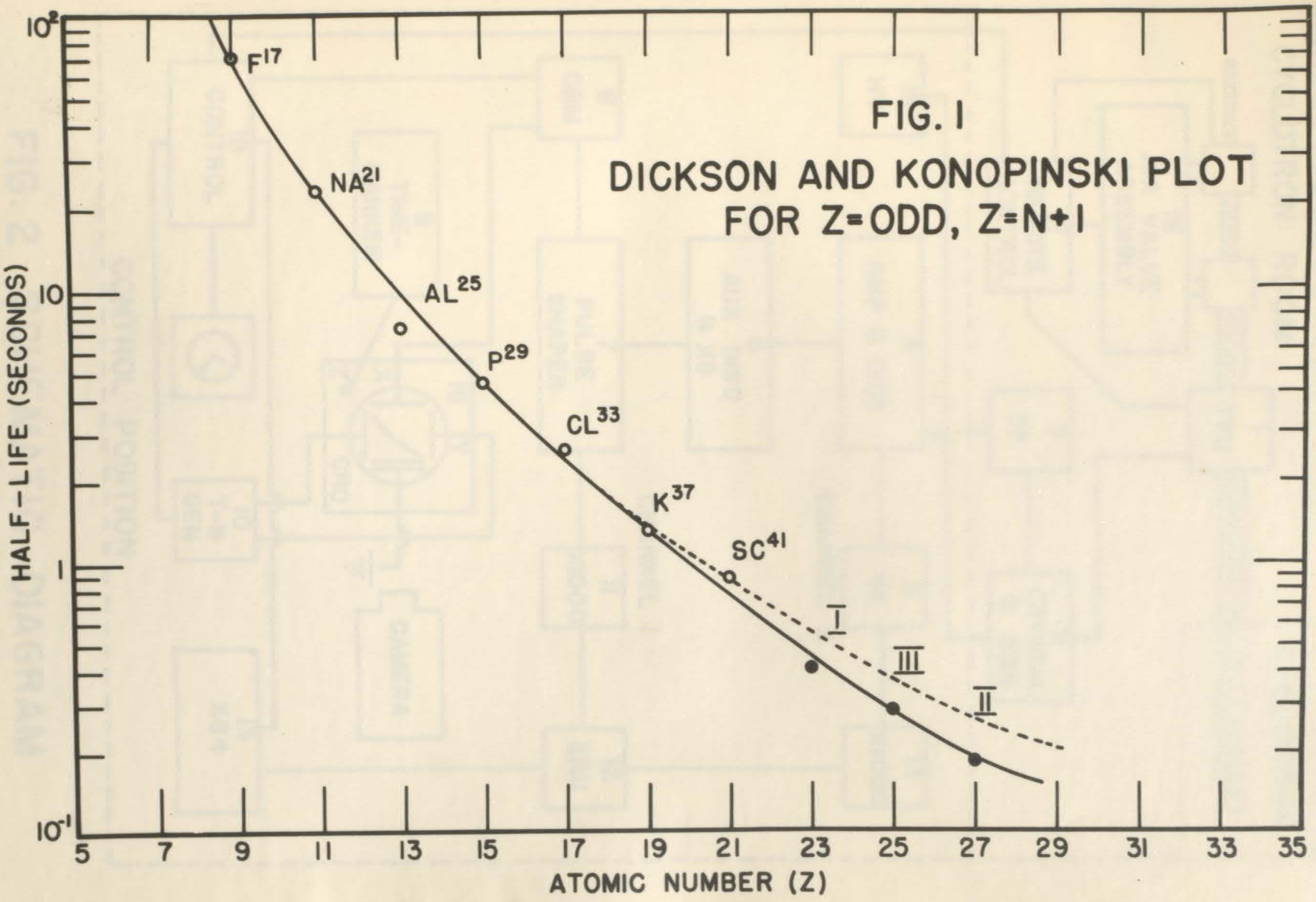
FIG. 1
DICKSON AND KONOPINSKI PLOT
FOR Z=ODD, Z=N+1
HALF-LIFE (SECONDS)
ATOMIC NUMBER (Z)
10^2
10
1
10^{-1}
5
7
9
11
13
15
17
19
21
23
25
27
29
31
33
35
F^{17}
NA^{21}
AL^{25}
P^{29}
CL^{33}
K^{37}
SC^{41}
I
III
II

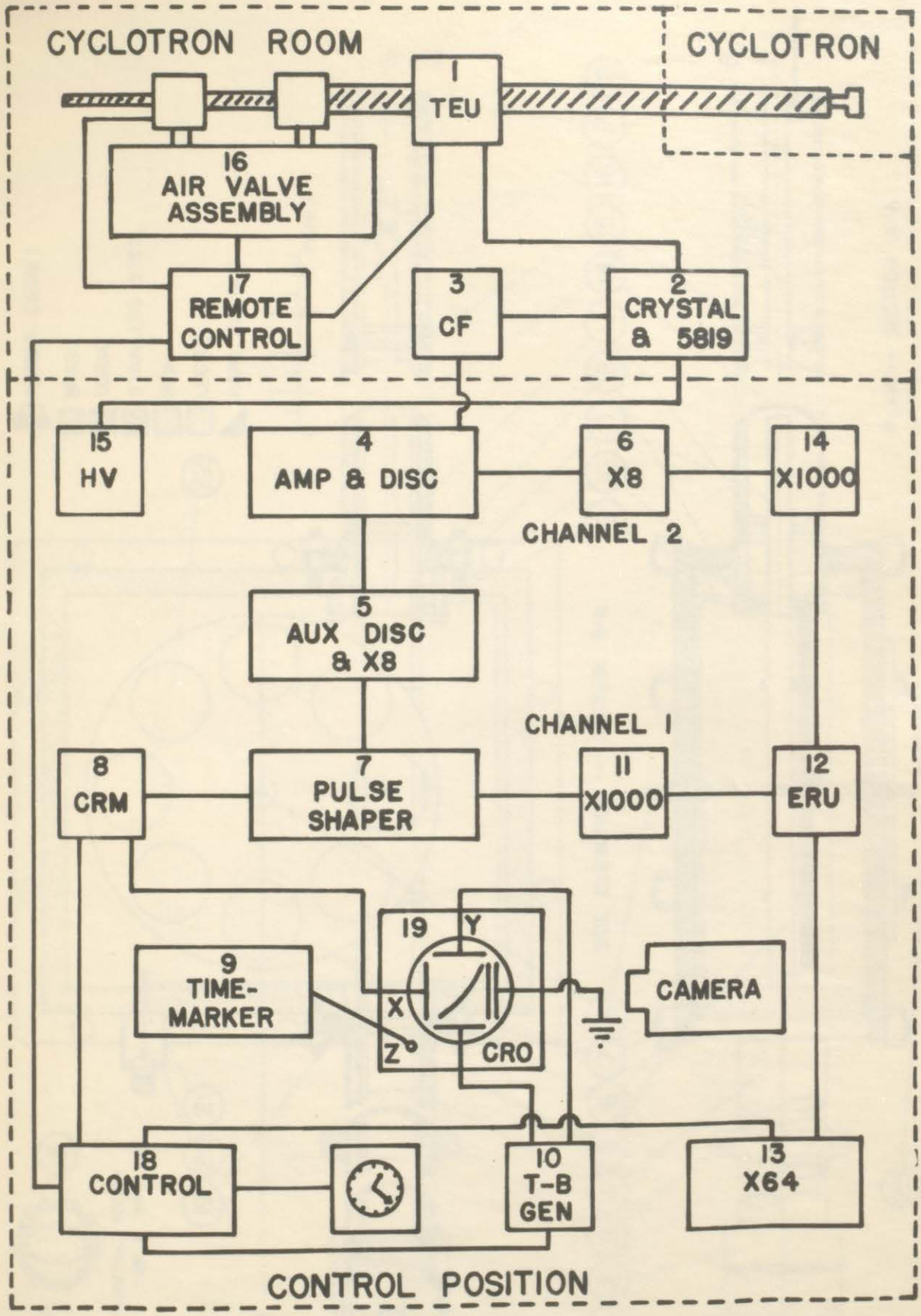

FIG. 2 SCHEMATIC DIAGRAM

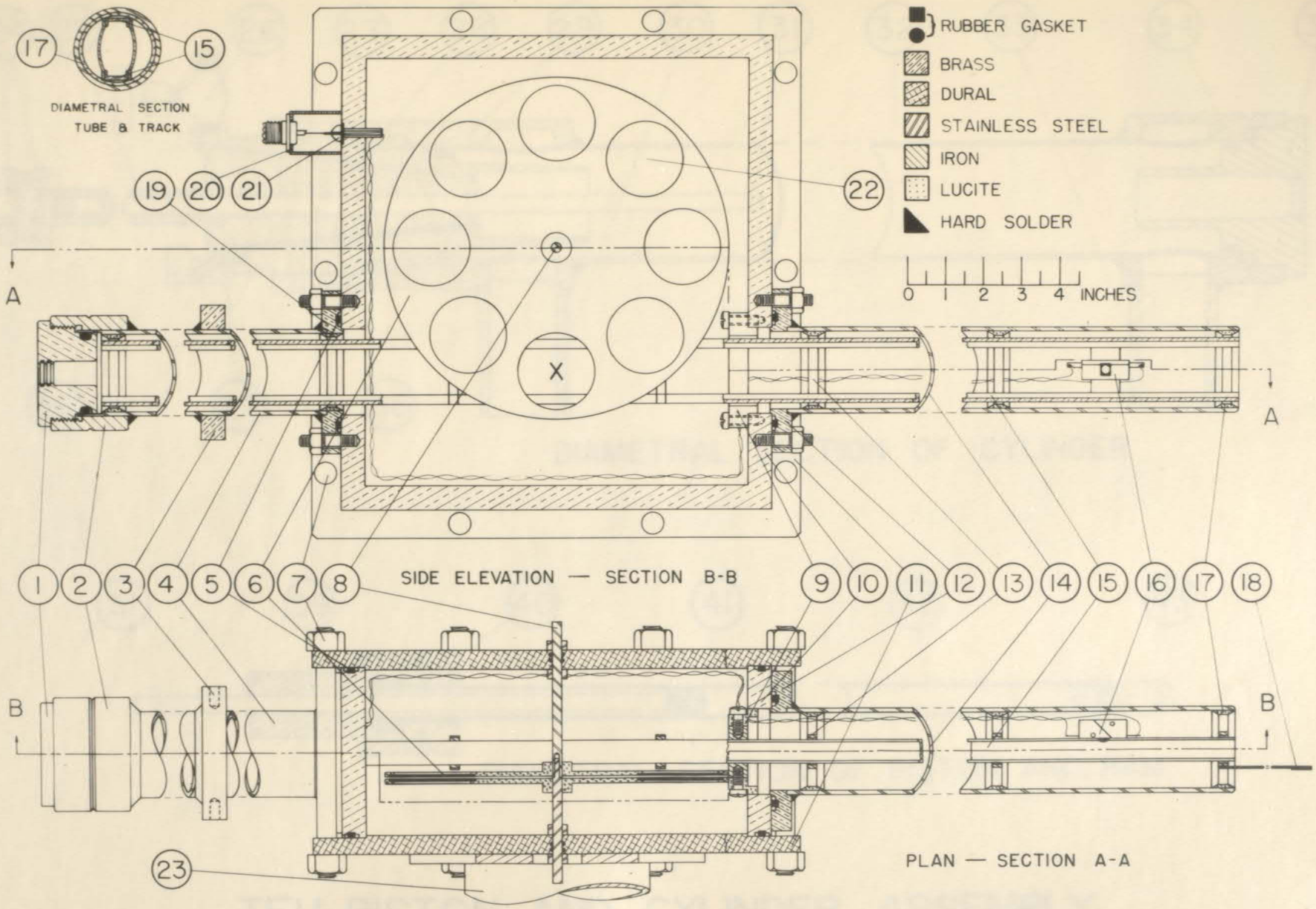

FIG. 3 TEU PROBE ASSEMBLY

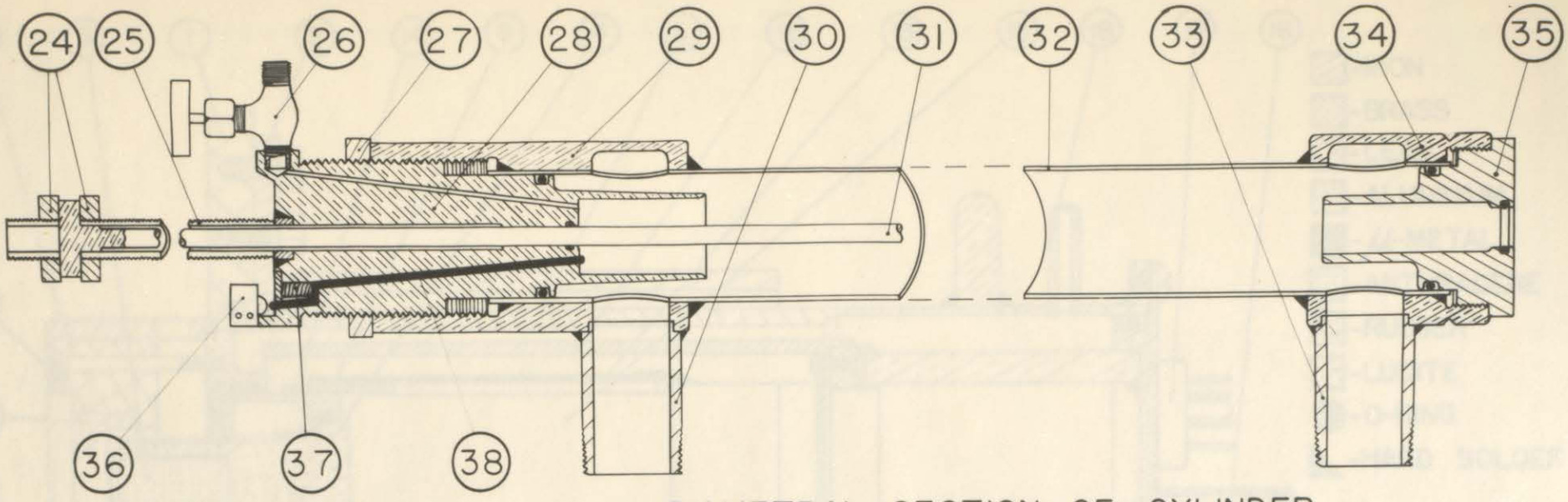

DIAMETRAL SECTION OF CYLINDER

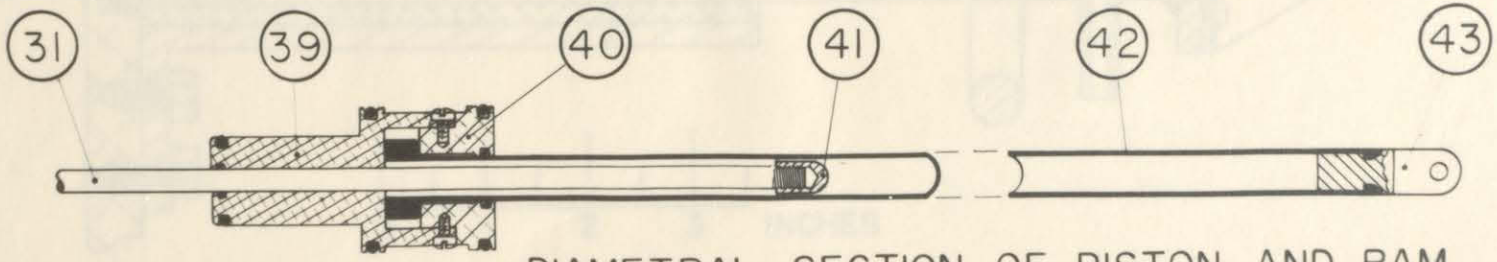

DIAMETRAL SECTION OF PISTON AND RAM

TEU-PISTON AND CYLINDER ASSEMBLY

FIG. 4

0 1 2 3 INCHES

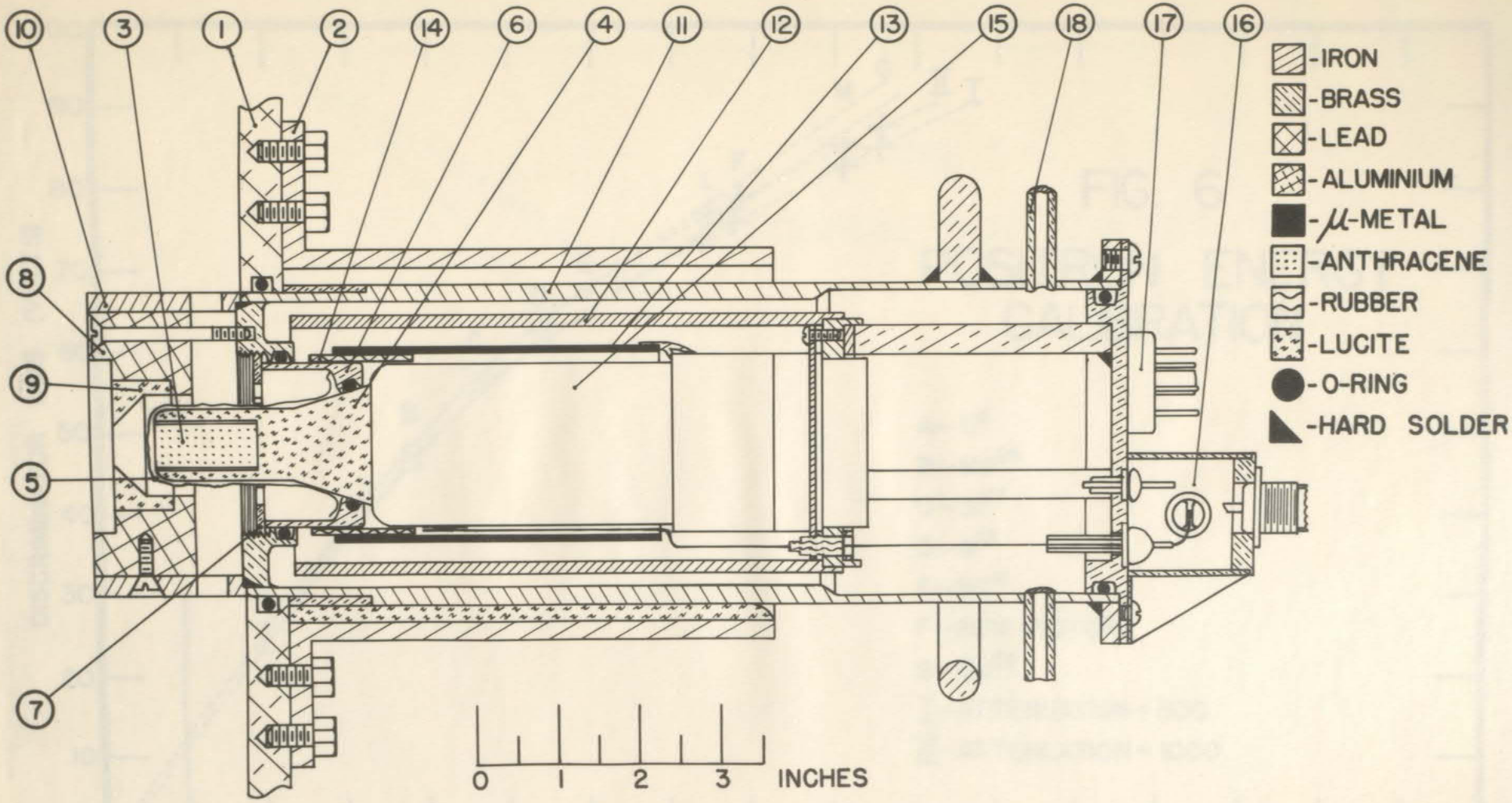

DIAMETRAL SECTION, SCINTILLATION COUNTER UNIT

FIG. 5

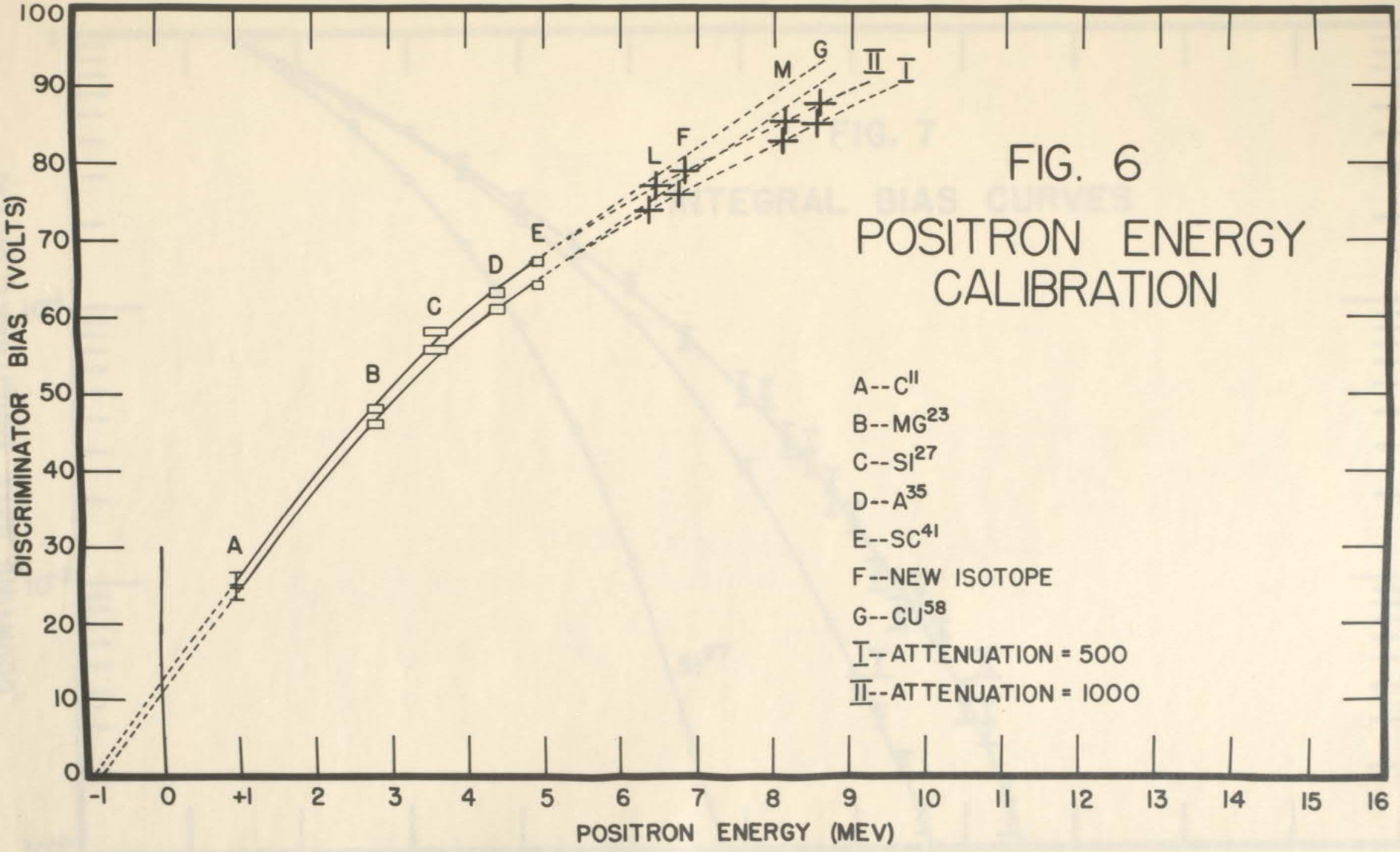
FIG. 6
POSITRON ENERGY CALIBRATION
A--C11
B--MG23
C--SI27
D--A35
E--SC41
F--NEW ISOTOPE
G--CU58
I--ATTENUATION = 500
II--ATTENUATION = 1000
DISCRIMINATOR BIAS (VOLTS)
POSITRON ENERGY (MEV)
0
10
20
30
40
50
60
70
80
90
100
-1
0
+1
2
3
4
5
6
7
8
9
10
11
12
13
14
15
16
A
B
C
D
E
F
G
L
M
I
II

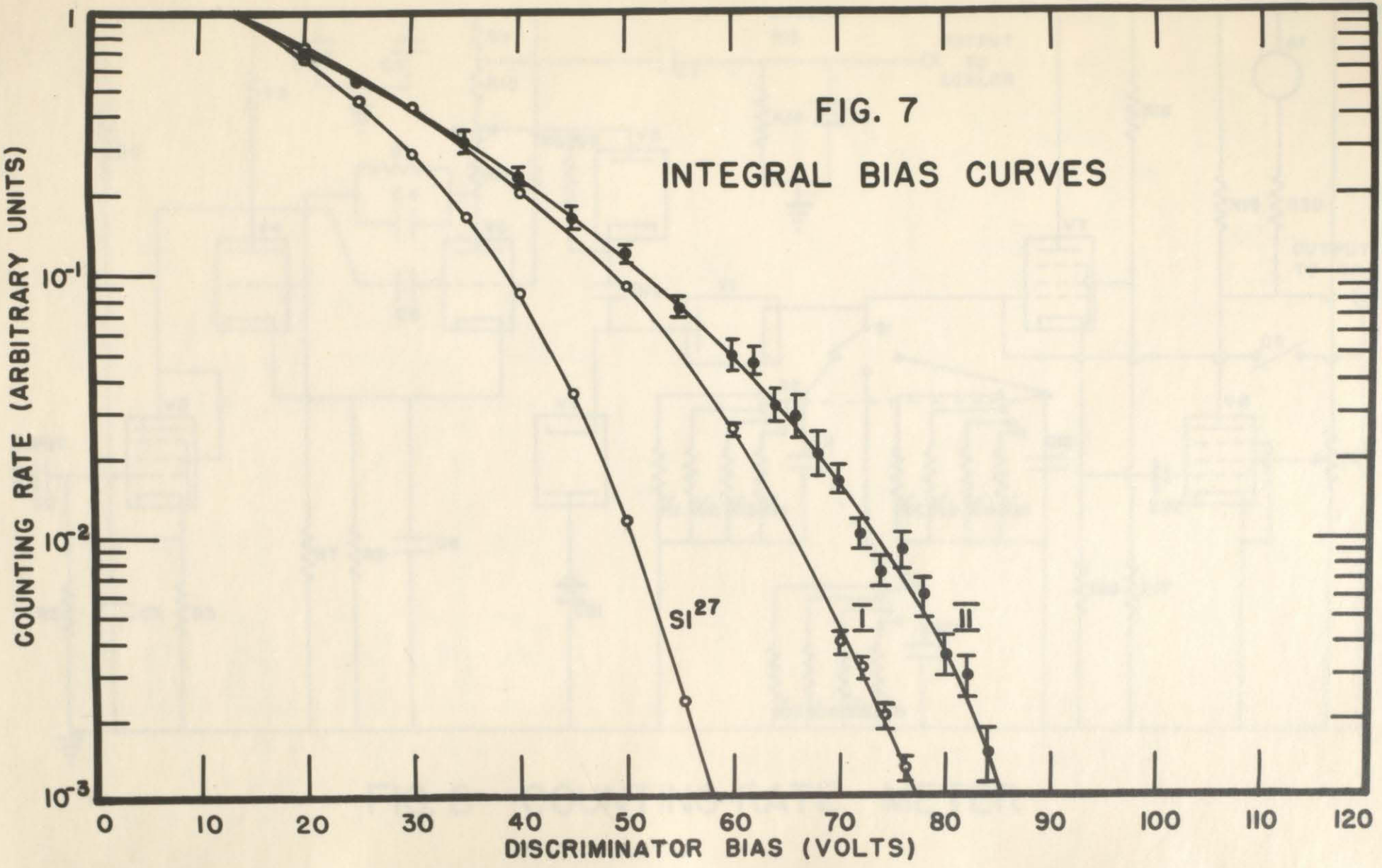
FIG. 7
INTEGRAL BIAS CURVES
COUNTING RATE (ARBITRARY UNITS)
1
10^{-1}
10^{-2}
10^{-3}
Si^{27}
I
II
0
10
20
30
40
50
60
70
80
90
100
110
120
DISCRIMINATOR BIAS (VOLTS)

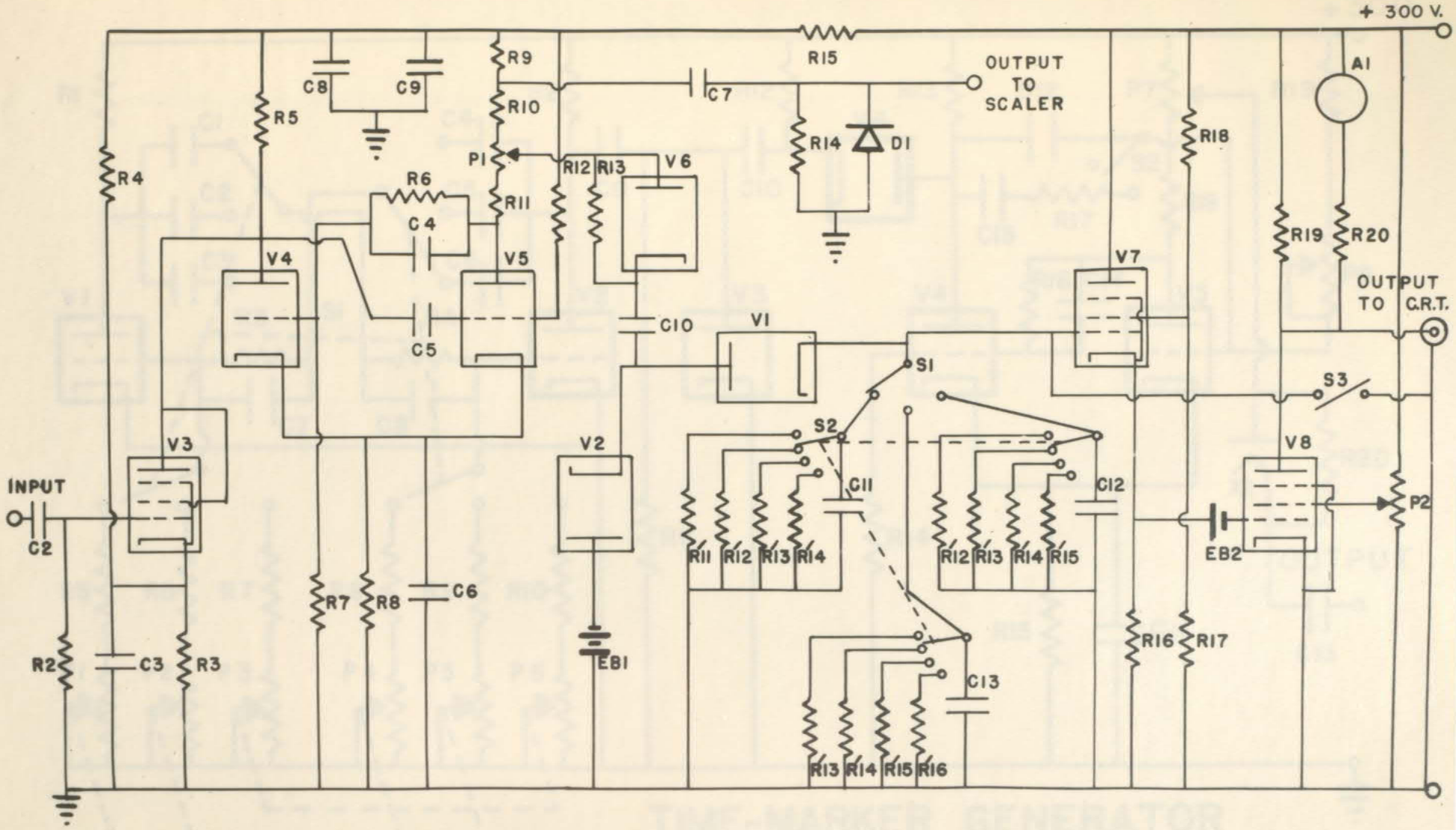

FIG. 8 COUNTING-RATE METER

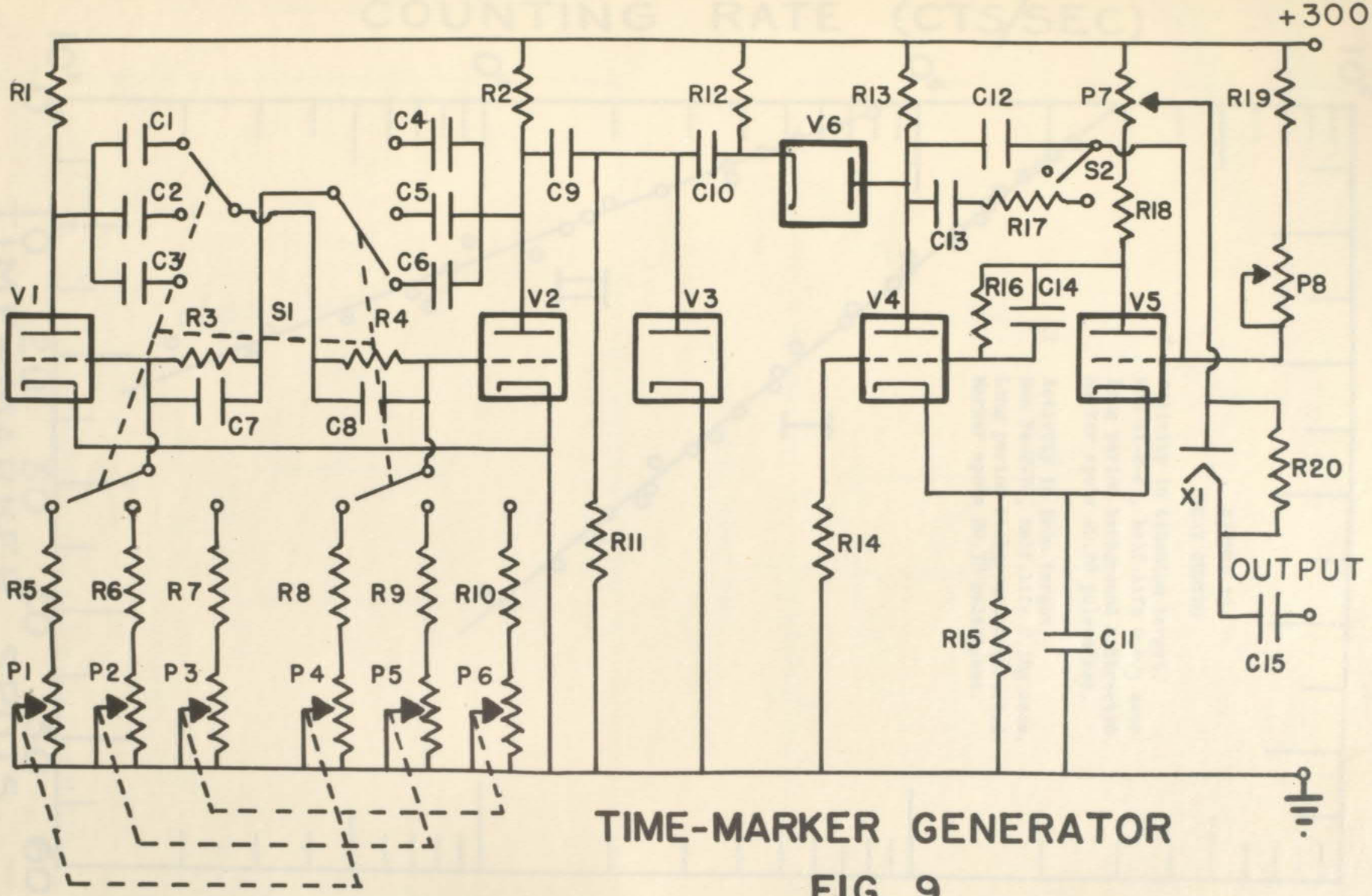

TIME-MARKER GENERATOR

FIG. 9

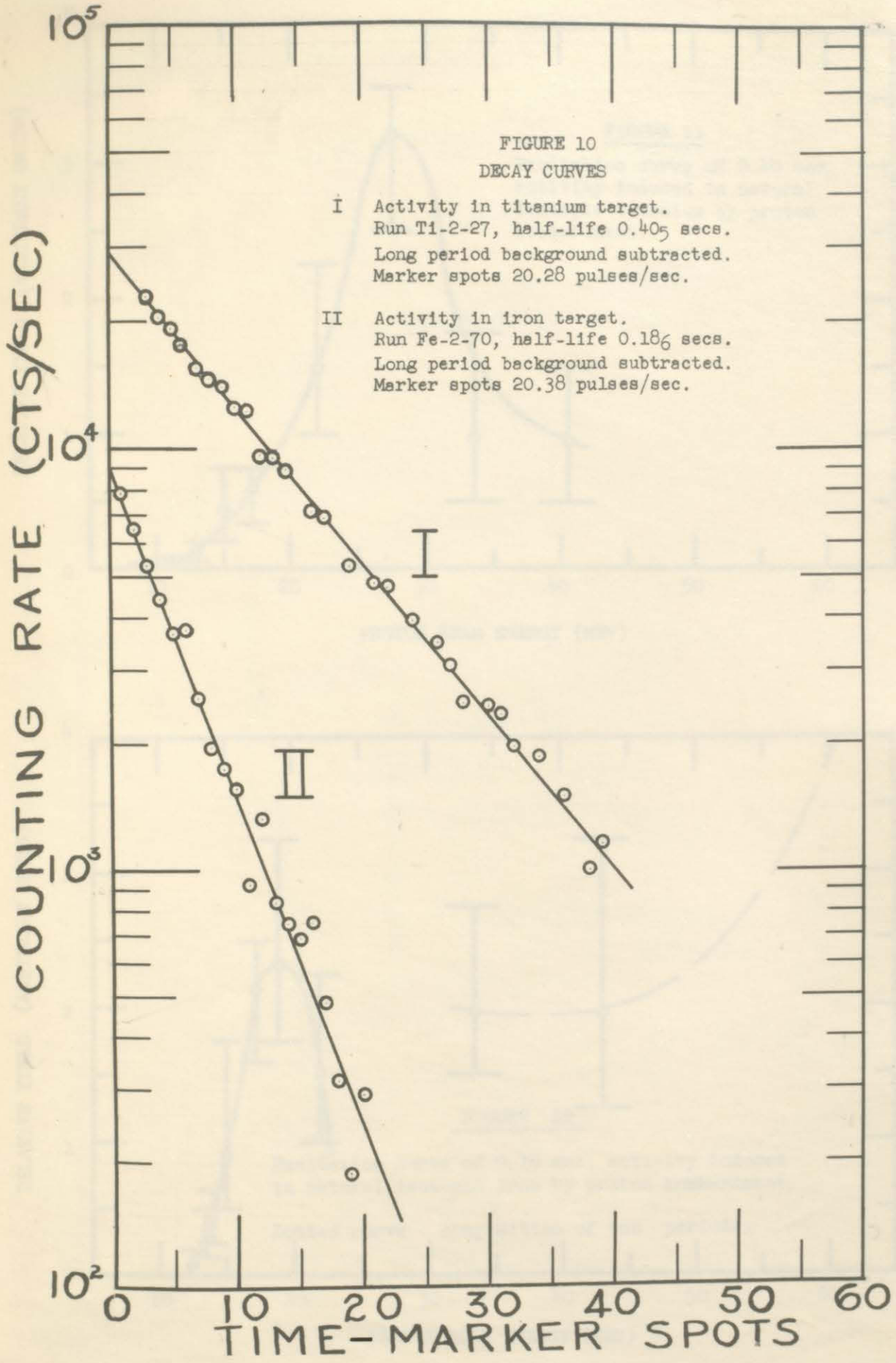
FIGURE 10
DECAY CURVES
I Activity in titanium target.
Run Ti-2-27, half-life 0.405 secs.
Long period background subtracted.
Marker spots 20.28 pulses/sec.
II Activity in iron target.
Run Fe-2-70, half-life 0.186 secs.
Long period background subtracted.
Marker spots 20.38 pulses/sec.
COUNTING RATE (CTS/SEC)
10^5
10^4
10^3
10^2
I
II
0
10
20
30
40
50
60
TIME-MARKER SPOTS

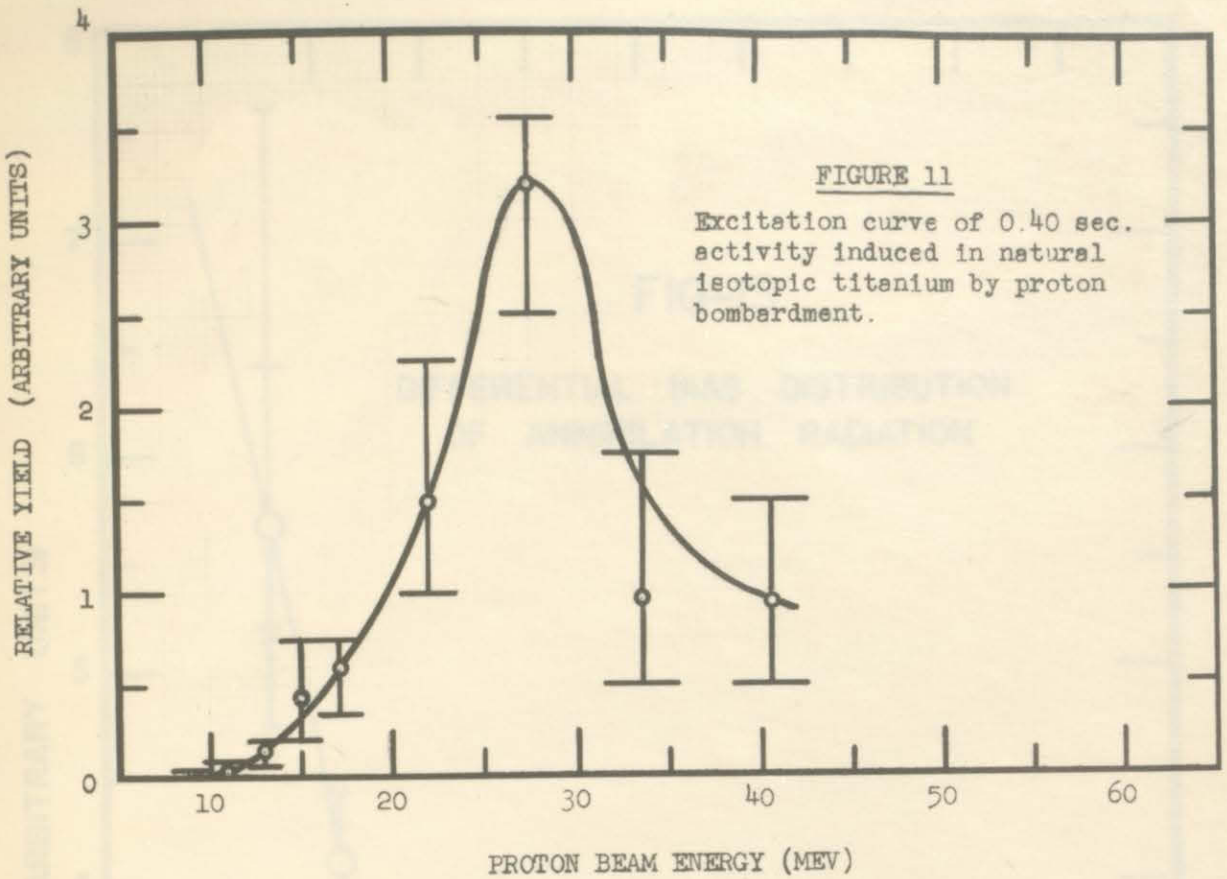

FIGURE 11

Excitation curve of 0.40 sec. activity induced in natural isotopic titanium by proton bombardment.

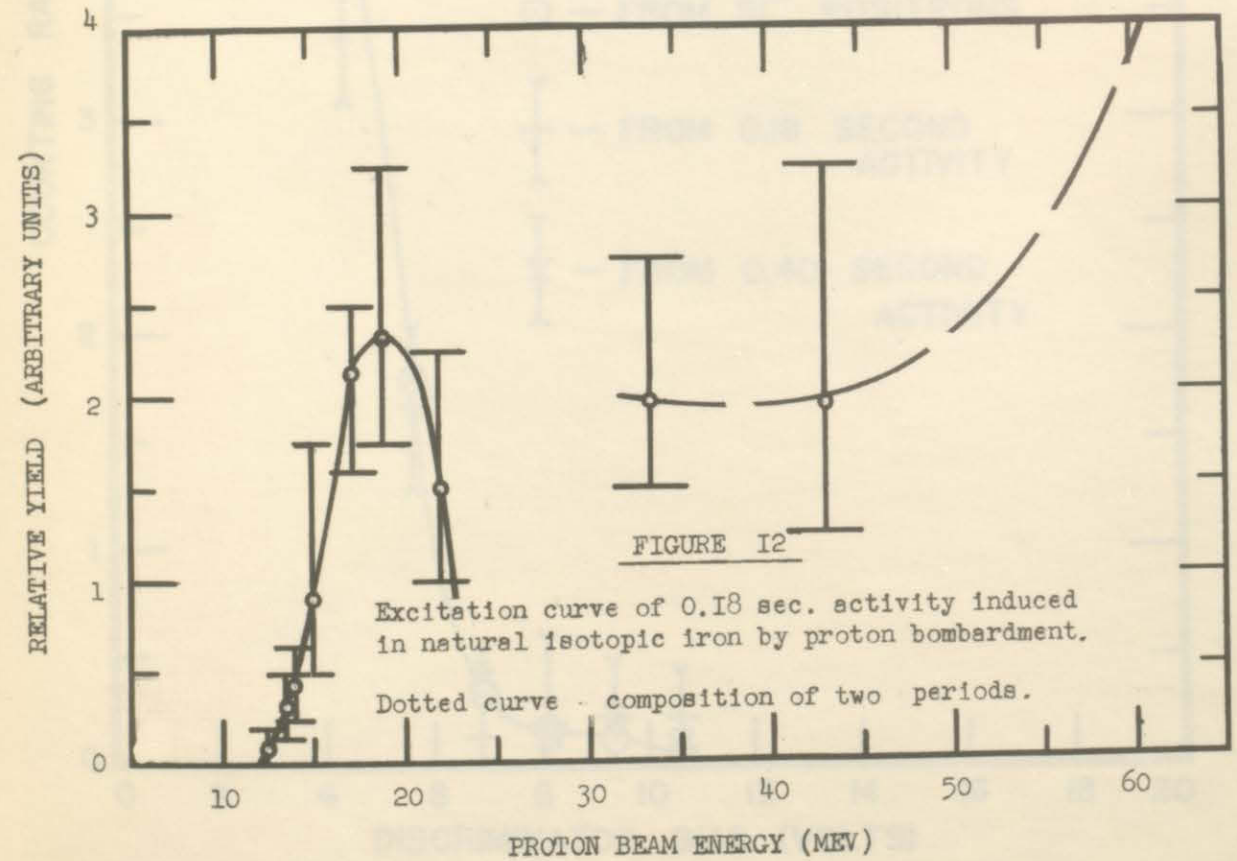

FIGURE I2

Excitation curve of 0.I8 sec. activity induced in natural isotopic iron by proton bombardment.

Dotted curve - composition of two periods.

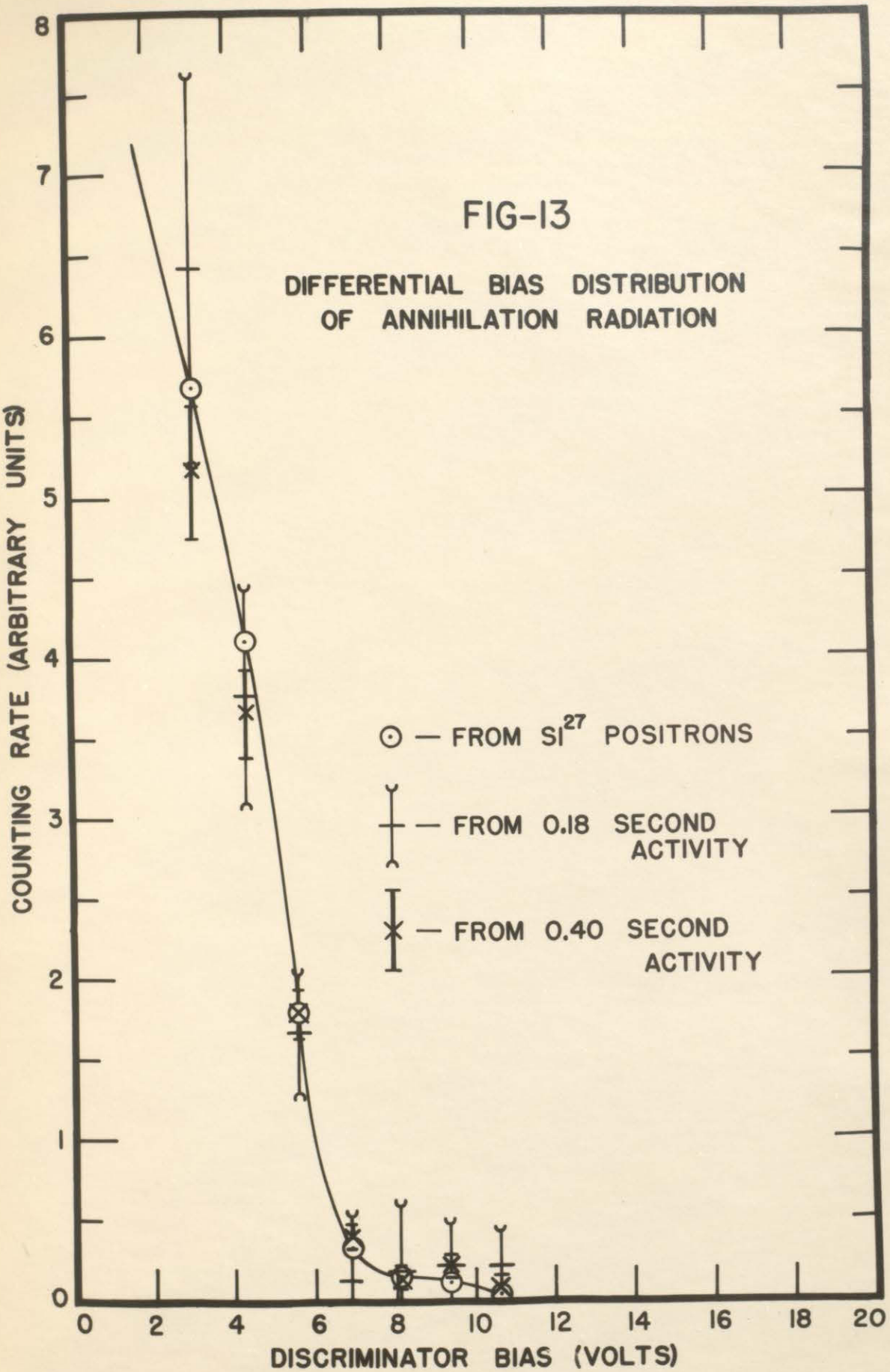
FIG-13
DIFFERENTIAL BIAS DISTRIBUTION
OF ANNIHILATION RADIATION
COUNTING RATE (ARBITRARY UNITS)
DISCRIMINATOR BIAS (VOLTS)
⊙ — FROM Si27 POSITRONS
— FROM 0.18 SECOND ACTIVITY
— FROM 0.40 SECOND ACTIVITY
0
1
2
3
4
5
6
7
8
0
2
4
6
8
10
12
14
16
18
20